Journal of Medicinal Chemistry

Article

Discovery of 8-Trifluoromethyl-3-cyclopropylmethyl-7-[(4-(2,4-difluorophenyl)-1-piperazinyl)methyl]-1,2,4-triazolo[4,3-a]pyridine (JNJ-46356479), a Selective and Orally Bioavailable mGlu2 receptor Positive Allosteric Modulator (PAM)

José María Cid, Gary Tresadern, Juan Antonio Vega, Ana Isabel de Lucas, Alcira del Cerro, Encarnación Matesanz, María Lourdes Linares, Aránzazu García, Laura Iturrino, Laura Pérez-Benito, Gregor J. Macdonald, Daniel Oehlrich, Hilde Lavreysen, Luc Peeters, Marc Ceusters, Abdellah Ahnaou, Wilhelmus Drinkenburg, Claire Mackie, Marijke Somers, and Andrés A. Trabanco

J. Med. Chem., **Just Accepted Manuscript** • DOI: 10.1021/acs.jmedchem.6b00913 • Publication Date (Web): 31 Aug 2016

Just Accepted

ACS Publications

Journal of Medicinal Chemistry is published by the American Chemical Society. 1155 Sixteenth Street N.W., Washington, DC 20036

Discovery of 8-Trifluoromethyl-3-cyclopropylmethyl-7-[(4-(2,4-difluorophenyl)-1-piperazinyl)methyl]-1,2,4-triazolo[4,3-a]pyridine (JNJ-46356479), a Selective and Orally Bioavailable mGlu2 receptor Positive Allosteric Modulator (PAM)

Jose María Cid,[a,] Gary Tresadern,[a] Juan Antonio Vega,[a] Ana Isabel de Lucas,[a] Alcira del Cerro,[a] Encarnación Matesanz,[a] María Lourdes Linares,[a] Aránzazu García,[a] Laura Iturrino,[a] Laura Pérez-Benito,[c] Gregor J. Macdonald,[b] Daniel Oehlrich,[b] Hilde Lavreysen,[b] Luc Peeters,[b] Marc Ceusters,[b] Abdellah Ahnaou,[b] Wilhelmus Drinkenburg,[b] Claire Mackie,[b] Marijke Somers,[b] Andrés A. Trabanco[a,*]*

[a]Janssen Research & Development, a division of Janssen-Cilag, S.A., Janssen-Cilag, Toledo, Spain.

[b]Janssen Research & Development, Janssen Pharmaceutica NV, Beerse, Belgium.

[c]Laboratori de Medicina Computacional Unitat de Bioestadistica, Facultat de Medicina, Universitat Autonoma de Barcelona, Bellaterra, Spain.

RECEIVED DATE (to be automatically inserted after your manuscript is accepted if required according to the journal that you are submitting your paper to)

ABSTRACT: Positive allosteric modulators of the metabotropic glutamate 2 receptor have generated great interest in the last decade. There is mounting evidence of their potential as therapeutic agents in the treatment of multiple central nervous system disorders. We have previously reported substantial efforts leading to potent and selective mGlu2 PAMs. However, finding compounds with the optimal combination of in vitro potency and good drug-like properties has remained elusive, in part because of the hydrophobic nature of the allosteric binding site. Herein, we report on the lead optimization process to overcome the poor solubility inherent to the advanced lead **6**. Initial prototypes already showed significant improvements in solubility while retaining good functional activity but displayed new liabilities associated to metabolism and hERG inhibition. Subsequent subtle modifications efficiently addressed those issues leading to the identification of compound **27** (JNJ-46356479). This new lead represents a more balanced profile that offers a significant improvement on the druglike attributes compared to previously reported leads.

KEYWORDS Allosteric modulators, mGlu2, mGluR2, GRM2, PAMs, metabotropic glutamate receptor, GPCR, class C GPCR, schizophrenia, anxiety, depression, sleep wake architecture, REM sleep, antipsychotic, homology model, molecular dynamics.

INTRODUCTION

The metabotropic glutamate 2 (mGlu2) receptor, which belongs to the group II subfamily of metabotropic glutamate (mGlu) receptors along with the mGlu3 receptor, has proven to be of particular interest in neuropharmacology.[1,2] It is widely distributed in the brain and is preferentially expressed on presynaptic nerve terminals, where it negatively modulates glutamate and GABA release.[3] High levels of mGlu2 receptors can be found in brain areas such as prefrontal cortex, hippocampus and amygdala where glutamate hyperfunction may be implicated in disorders and diseases such as anxiety, schizophrenia[4,5] and chronic pain.[6,7]

Clinical data have become available for several mixed mGlu2/3 agonists in anxiety and schizophrenia. Thus, (+)-2-aminobicyclo[3.1.0]hexane-2,6-dicarboxylic acid (**1**, LY354740, Figure 1)[8] was found to have anxiolytic efficacy in healthy volunteers showing activity in fear-potentiated startle and panic induction after CO2 challenge.[9] (1S,2*S*,5*R*,6S)-2-[(2'*S*)-(2'-Amino)propionyl]aminobicyclo[3.1.0] hexane-2,6-dicarboxylic acid (**2**, LY544344),[10] a prodrug of **1**, showed significant anxiolytic effects in a clinical trial with patients suffering from generalized anxiety disorder (GAD). Treatment with **2** resulted in a significant improvement from baseline in Hamilton Anxiety and Clinical Global Impression Scores as well as in remission rates compared to placebo. Unfortunately this trial was discontinued in an early stage based on findings of convulsions in preclinical studies.[11] In addition, Phase IIb clinical data have been reported for [(1*R*,4*S*,5*S*,6*S*)-2-thiabicyclo[3.1.0]-hexane-4,6-dicarboxylic acid,4-[(2*S*)-2-amino-4-(methylthio)-1-oxobutyl]amino- 2,2-dioxide monohydrate (**3**, LY2140023, pomaglumetad methionil),[12] a prodrug of the mixed mGu2/3 agonist (−)-(1*R*,4*S*,5*S*,6*S*)-4-amino-2-sulfonylbicyclo[3.1.0]hexane-4,6-dicarboxylic acid (LY404039),[13] showing improvement of both positive and negative symptoms in schizophrenic patients.[14] However, in 2012 the originating company announced the decision to stop the Phase III clinical trials of **3** for the treatment of patients suffering from schizophrenia.[15,16] Moreover, a very recent analysis has shown that **3** is effective in subgroups of schizophrenic patients that are early in disease and had not been treated with atypical

antipsychotic antagonizing 5-HT2A receptors but had been treated with classical antipsychotics antagonizing D2 receptors.[17]

Given the interest in mGlu2 receptor activation, attention has turned towards the search for selective mGlu2 receptor positive allosteric modulators as an alternative approach to enhance endogenous glutamate agonist response with little or no intrinsic activity. The fact that allosteric modulators bind at an alternative site to orthosteric agonists offers multiple potential benefits: opportunity to access a novel chemical space, potential for improved selectivity versus other members of the mGlu family, and lower potential for receptor desensitization and tolerance because PAMs function only in the presence of physiologically controlled levels of glutamate. To date, multiple series of selective mGlu2 receptor PAMs have been described,[18-20] and two of them have entered the clinic: 7-methyl-5-[3-(piperazin-1-ylmethyl)-1,2,4-oxadiazol-5-yl]-2-[[4-(trifluoromethoxy)phenyl]methyl]-3*H*-isoindol-1-one (**4**, AZD8529)[21] from AstraZeneca and 1-butyl-3-chloro-4-(4-phenyl-1-piperidinyl)-(1*H*)-pyridone (**5**, JNJ-40411813, also known as ADX71149) from Janssen Pharmaceuticals, Inc. (Janssen) and Addex Therapeutics (Addex). Compound **4** (Figure 1) advanced into phase II clinical trials in schizophrenic patients in 2009[22] but it was discontinued in early 2011 due to lack of efficacy.[23] Currently **4** is in the recruiting phase for a phase II clinical trial to study smoking cessation in female smokers.[24]

In an exploratory phase IIa study in schizophrenia, compound **5** met the primary objectives of safety and tolerability. Moreover, patients treated with antipsychotics who experience residual negative symptoms were identified as the subgroup that may potentially benefit from add-on treatment with **5**, although this is yet to be established in a formal proof-of-concept study.[25] In addition, in a second phase IIa study with **5** as adjunctive therapy in patients having major depressive disorder with significant anxiety symptoms, **5** did not meet the criterion for efficacy *vs.* placebo.[26] Despite a lack of signal on the primary outcome measure, treatment with **5** showed efficacy signals on several anxiety measures and on all depression measures,[27] however overall the results do not suggest efficacy for **5** as an adjunctive treatment for patients with MDD with significant anxious symptoms.

To search for a more potent, efficacious and structurally differentiated back-up candidate to pyridone **5**, a scaffold-hopping drug-design strategy was carried out. Computational techniques based on 3D shape and electrostatic similarity led to the identification of a series of imidazopyridines[28-31] which evolved into the recently disclosed 1,2,4-triazolopyridines.[32,33] Structure activity relationship (SAR) studies resulted in the lead compound 3-cyclopropylmethyl-7-(4-phenyl-piperidin-1-yl)-8-trifluoromethyl[1,2,4]triazolo[4,3a] pyridine (**6**, JNJ-42153605)[32] as a potent and selective mGlu2 receptor PAM with an acceptable pharmacokinetic profile in rodent and non-rodent species (Figure 1). Compound **6** showed centrally mediated in vivo effectivity in models sensitive to mGlu2 receptor modulation such as sleep-wake electro encephalogram (sw-EEG) in rats,[34] showing suppressed REM sleep during the first four hours after oral administration of a 3 mg/kg dose. However, **6** showed limited solubility in water (< 0.004 mg/mL) and pH 4 buffer containing 20% HP-β-cyclodextrin (0.995 mg/mL), which could hinder its further development. These deficiencies were initially predicted by our kinetic solubility assay, where **6** presented solubility values lower than 0.8 μM at pH 4 and 7. We hypothesized that placing a methylene spacer between the piperidine ring and the triazole core (**A**, Figure 1) would generate a basic center and hence improve aqueous solubility. This strategy delivered a new potent, selective, soluble, orally bioavailable triazolopyridine class, the subject of this report. An extensive profiling of the most advanced lead 8-trifluoromethyl-3-cyclopropylmethyl-7-[(4-(2,4-difluorophenyl)-1-piperazinyl)methyl]-1,2,4-triazolo[4,3-a]pyridine (**27**, JNJ-46356479) which overcomes deficiencies associated with **6** is also discussed.

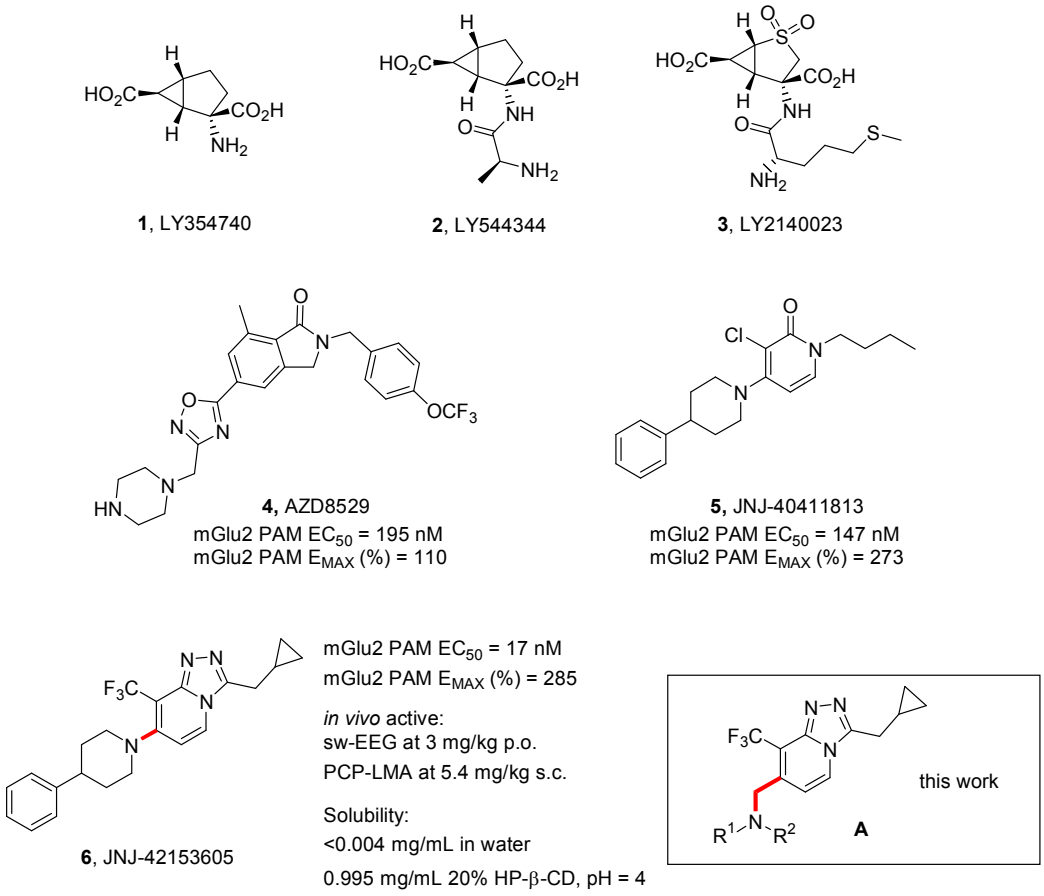

Figure 1. Representative mGlu2 receptor orthosteric agonists and PAMs. Previous key leads **5** and **6** are shown, along with schematic **A** describing the subject of this study with NR^1R^2 groups shown in Table 1.

As shown in Scheme 1, the synthesis of C-7 aminomethylene triazolopyridine derivatives **6-23** were prepared using two alternative procedures. The key intermediate **3** was obtained from the 7-chlorotriazolopyridine **1**,[32] followed by Suzuki cross coupling to introduce a vinyl group and subsequent oxidative rupture of the double bond in **2** to afford the aldehyde intermediate **3.** Final compounds **6-23** were prepared either by reductive amination with $NaBH(OAc)_3$ or by a two-step synthesis starting with a reduction of the carbonyl function in **3** with $NaBH_4$, followed by reaction of **4** with mesyl chloride leading to intermediate **5** which was then transformed into the corresponding target compounds by nucleophilic substitution reaction with the corresponding amines.

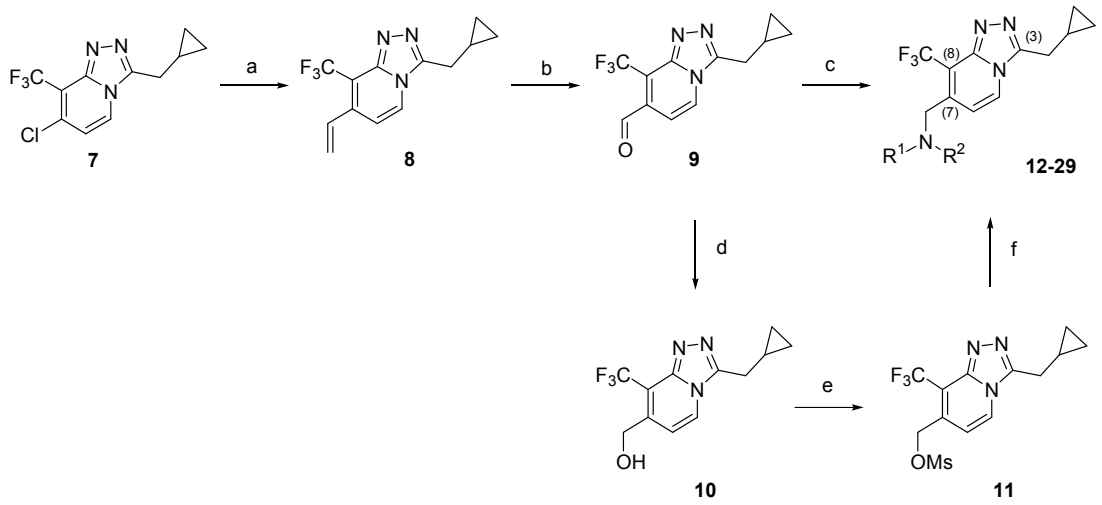

Scheme 1. Reagents and conditions: (a) 4,4,5,5-tetramethyl-2-vinyl-1,3,2-dioxoborolane, $Pd(PPh_3)_4$, 1,4-dioxane, aq. $NaHCO_3$, 100 ºC, 18 h, 94 %; (b) OsO_4, $NaIO_4$, 1,4-dioxane/H_2O, rt, 2 h, 60 %; (c) amine, $NaBH(OAc)_3$, AcOH, DCE, rt, 16h, 18 – 64%; (d) $NaBH_4$, MeOH, 0 ºC, 1 h, 81 %; (e) MsCl, NEt_3, CH_2Cl_2, rt, 2 h, 84 % ; (f) amine, DIPEA, CH_3CN, 80-90 ºC, 1 - 4 h, 6 – 60 %.

Representative compounds of this C-7 aminomethylene triazolopyridine series (**12**-**29**) are shown in Table 1 along with mGlu2 PAM functional activity, kinetic solubility, human and rat metabolic stability and hERG patch-clamp data. In general, the introduction of the methylene spacer between the triazolopyridine core and the cyclic amine was beneficial for the kinetic solubility of the molecules while not being detrimental for their functional activity. However this improved solubility was accompanied by diminished metabolic stability in rat liver microsomes (RLM) and enhanced hERG channel inhibition. These trends were observed for the vast majority of compounds prepared within this series. As such the identification of a lead combining all the desired properties was not initially straight forward.

By way of example, 3-(cyclopropylmethyl)-7-[(4-phenylpiperidin-1-yl)methyl]-8-(trifluoromethyl)-[1,2,4]triazolo[4,3-a]pyridine (**12**, also known as JNJ-46281222)[35], the direct analogue of **6**, showed much improved solubility in the kinetic solubility assay at pH 4 and 7 and displayed equipotent activity (**12**: EC_{50} = 21 nM *vs* **6**: EC_{50} = 17 nM) in the mGlu2 receptor functional assay. Unfortunately **12** was

found to be unstable in RLM (84% metabolized after 15 minutes incubation at 5μM) and showed strong inhibition (83%) of the hERG channel at 3 μM. The introduction of additional substituents at position C-4 of the piperidine ring (**13**-**15**) was detrimental for mGlu2 PAM potency and did not result in improved metabolic stability in RLM. Shifting of the phenyl group from position C-4 to position C-3 of the piperidine ring (**16**) did not improve the overall profile of the molecule. Of note is that an additional methyl substituent at C-3 position (**17**) gave a remarkable increase in potency, with a mGlu2 PAM EC_{50} ~3 nM; however both **16** and **17** showed poor metabolic stability in HLM and RLM, which halted further exploration of the 3-phenylpiperidine moiety. The introduction of halogen atoms in the 4-phenyl substituent of the piperidine ring (**18**-**20**) led to a slight increase in potency, but these analogues still showed high metabolism in RLM and strong inhibition of the hERG channel. Reduction of metabolism and diminished hERG channel inhibition was also observed for **21** which contains the 2,4-difluorophenyl substituent attached to the C4-position of the piperidine ring. Compounds **22** and **23**, containing a spacer between the 2,4-difluorophenyl and piperidine ring, were nearly 4-fold less potent than **21** and showed higher metabolic instability in both HLM and RLM. The 4-(2,4-difluorophenyl)cyclohexylamine derivatives **24** and **25** were also found to be either metabolically unstable (**24**) or show a hERG liability (**25**). Replacement of the piperidine ring by a piperazine was detrimental for activity and thus compounds **26** and **27** were ~2.6- and ~5-fold less potent than their corresponding piperidine counterparts **18** and **19**. Compound **27** also combined good kinetic solubility and microsomal stability, and moreover it only showed 30 % inhibition of the hERG channel at 3 μM concentration. Although replacement of the aromatic fluorine atoms in **27** by the more lipophilic chlorine atoms in **28** led to a potency increase (**28**: EC_{50} = 17 nM vs **27**: EC_{50} = 78 nM) the inhibition of the hERG channel was also increased for the latter compound (**28**: hERG = 86 % inh.). Good primary activity was also found for the homopiperazine analogue (**29**) of compound **27**, however, this potency increase came together with high metabolic instability in HLM and RLM. The calculated basicity (pKa)

was highest for molecules such as **25**, **27** and **28** which had better HLM and RLM. However, this alone is insufficient because **26** and **29** have similarly higher basicity but poor metabolic stability.

Table 1. mGlu2 PAM functional activity, kinetic solubility, human and rat metabolic stability and hERG patch-clamp data of representative C-7 aminomethylene triazolopyridine mGlu2 receptor PAMs **12**-**29**.

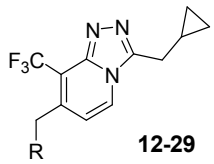

12-29

Compd	R	pK_a (calc.)[a]	mGlu2 EC_{50} (nM)[b]	mGlu2 E_{max} (%)[b]	Kin sol (μM) pH4/pH7[c]	HLM (%)[d]	RLM (%)[d]	hERG *(% inh. @ 3 μM)*
5	--	1.1	147	273	< 0.8 / < 0.8	23	53	51
6	--	3.1	17	285	< 0.8 / < 0.8	23	25	57
12	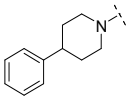	3.7	21	261	> 100 / 3	11	84	87
13	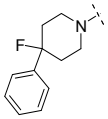	2.4	132	260	90 / 2	24	78	70
14	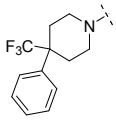	2.4	58	276	93 / 13	35	98	n.t.[e]
15	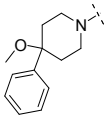	2.6	26	249	n.t.[e]/ n.t.[e]	69	98	n.t.[e]
16	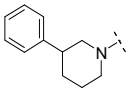	5.7	65	240	91 / 45	51	98	n.t.[e]
17	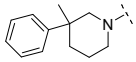	5.9	2.6	278	n.t.[e]/ n.t.[e]	97	99	n.t.[e]

18	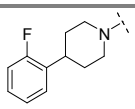	3.5	15	353	> 100 / 2	8	85	86
19	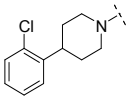	3.5	13.5	328	n.t. [e] / n.t. [e]	13	90	93
20	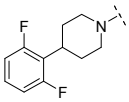	3.5	9.7	330	n.t. [e] / n.t. [e]	5	75	88
21	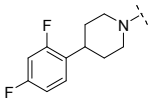	3.5	15	255	n.t. [e] / <0.6	6	9	69
22	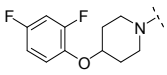	4.4	57	272	> 100 / 7	25	57	63
23	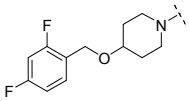	4.7	57	332	> 100 / 3	67	96	n.t. [e]
24	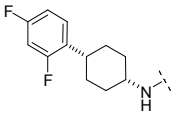	6.5	38	279	81 / 31.	81	84	n.t. [e]
25	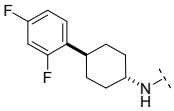	6.5	83	264	n.t. [e] / n.t. [e]	33	34	83
26	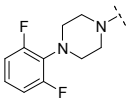	5.3	26	366	n.t. [e] / n.t. [e]	55	99	n.t. [e]
27	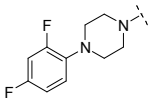	5.5	78	256	95 / 17	7	29	30
28	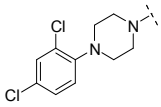	4.2	17	262	71 / 1	1	9	86
29	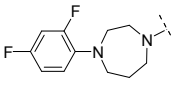	5.8	22	255	n.t. [e] / n.t. [e]	91	99	n.t. [e]

[a] Most basic pK_a calculated with ACS Labs v2014. [b] Values are means of at least two experiments and within Confidence Interval > 95%. [c] Compound concentrations were measured by UPLC/UV using a three point reference calibration and are means of at least two experiments. [d] HLM and RLM data refer to % of compound metabolized after 15 min at 5 μM concentration [e] n.t. Not tested.

Table 2. mGlu2 receptor PAM [^{35}S]-GTPγS functional activity of Glutamate, **27**, **5** and **6** on wild type and mutant receptors.

Compd	mGlu2 WT [a] (Transient [b]) EC_{50} (nM)	mGlu2 L639A EC_{50} (nM)	mGlu2 F643A EC_{50} (nM)	mGlu2 L732A EC_{50} (nM)	mGlu2 N735D EC_{50} (nM)	mGlu2 W773A EC_{50} (nM)	mGlu2 F776A EC_{50} (nM)
Glutamate [c]	5010	6310	10000	3980	6310	10000	5010
5	65	1350	2000	77	1630	2570	265
6	4.8	n.t. [d]	385	46.4	27.0	>10000	23.6
27	45.7	n.t. [d]	6610	977	1410	2340	n.t. [d]

Values are means of at least two experiments. See experimental Methods for more details. [a] WT wild type receptor. [b] All data including WT and mutants are for transiently transfected CHO-K1 cells, in contrast to stably transfected cells reported in Table 1. [c] Glutamate agonist EC_{50} (glutamate-induced [^{35}S]GTPγS binding). [d] n.t. Not tested

On the basis of these results, compound **27** displayed the best combination of mGlu2 PAM activity, good microsomal stability and low hERG liability within this series. It was pursued further with extensive characterization and comparison with the previous leads.

To further understand the in vitro SAR and binding at mGlu2 receptors, we performed binding displacement, mutagenesis and computational molecular modeling on the key leads. Radioligand binding studies using [^{3}H]-**12** as an allosteric mGlu2 receptor radioligand[35] showed that **27**, **5** and **6** fully displaced [^{3}H]-**12** with an K_i of 150, 180 and 15 nM respectively, suggesting these molecules share a common allosteric binding site. Experimental mutagenesis was performed analogous to previous work[33,36] (Table 2). Molecules **27**, **5** and **6** were affected by mutation of similar amino acids, such as F643$^{3.36a.40c}$, N735$^{5.47a.47.c}$ W773$^{6.48a.50c}$ implying the lead molecules make comparable receptor interactions and likely share a common allosteric binding site.

Molecules **27** and **6** were docked into an mGlu2 receptor homology model revealing a similar plausible binding mode that were consistent with the binding and mutagenesis experiments; see Figure 2A and Figure S1. They align in a parallel orientation to the alpha-helical segments of the 7-transmembrane domain with the cyclopropylmethyl triazolopyridine being oriented toward the

intracellular side of the receptor and interacting with a hydrophobic cluster formed by L639$^{3.32a.36c}$, F643$^{3.36a.40c}$, L732$^{5.43a.44c}$, and W773$^{6.48a.50c}$, some of which were important in the mutagenesis study. A triazolopyridine nitrogen of the ligand core accepts a hydrogen bond acceptor from N735$^{5.47a.47.c}$ and satisfies an important pharmacophoric feature of mGlu2 receptor PAMs.[28] The N735D mutation reduced activity suggesting this amino acid provides a hydrogen bond donor to the ligand. The main difference occurs towards the extracellular side, whereby the flexibility of **27** permits a more 'bent' orientation compared to the more linear orientation of **6**. This region of the receptor is more open, which is consistent with the structural diversity that is permitted on the C-7 substituents of the triazolopyridines (Table 1). Allosteric modulators of mGlu receptors typically form few H-bonds, and instead bind with steric and hydrophobic complementarity in a narrow binding site.[37] It is plausible that the increased potency of **6** compared to **27** comes from a combination of electrostatic and conformational differences between the piperidine and piperazine rings with the former showing higher activity for comparable analogues. Alternatively, the increased basicity of **27** compared to **6** (calculated pK_a of 5.5 and 3.1 respectively) may incur an extra desolvation cost contributing to its lower activity.

The stability and behavior of the binding mode for **27** was studied with molecular dynamics (MD) for a total of 3 (1+2 replicas) 1 microsecond simulations, in the presence of ligand, membrane, solvent and G-protein. The receptor was stable throughout the simulations showing little structural movement, Figure 2(B). The key hydrogen bond between N735$^{5.47a.47.c}$ and the ligand was maintained, Figure 2(C). Multiple amino acids around the ligand such as F643$^{3.36a.40c}$ showed only small fluctuations in their position, Figure 2(D). In contrast, W773$^{6.48a.50c}$ made a large inward movement (seen in all three simulations) in synergy with the cyclopropylmethyl of the ligand to form a hydrogen bond with Y647$^{3.39a.43c}$. The tryptophan is in a conserved motif (WLAFxPI) in transmembrane (TM) 6 in mGlu receptors, suggesting functional importance. Also, the 6.48a position is part of the TM6 transmission switch important for activation in class A GPCRs. Ligand induced movement of this amino acid may be a source of functional activity of mGlu2 PAMs. Compared to the MD simulations performed for **6**,[35]

here we have run the simulations for a further 500 ns, reaching a full microsecond. The results reveal consistent behavior adding further evidence to the behavior of PAMs of this chemical series. Overall, the docking and MD simulations confirmed a stable binding mode agreeing with experimental data for **27** and **6**.

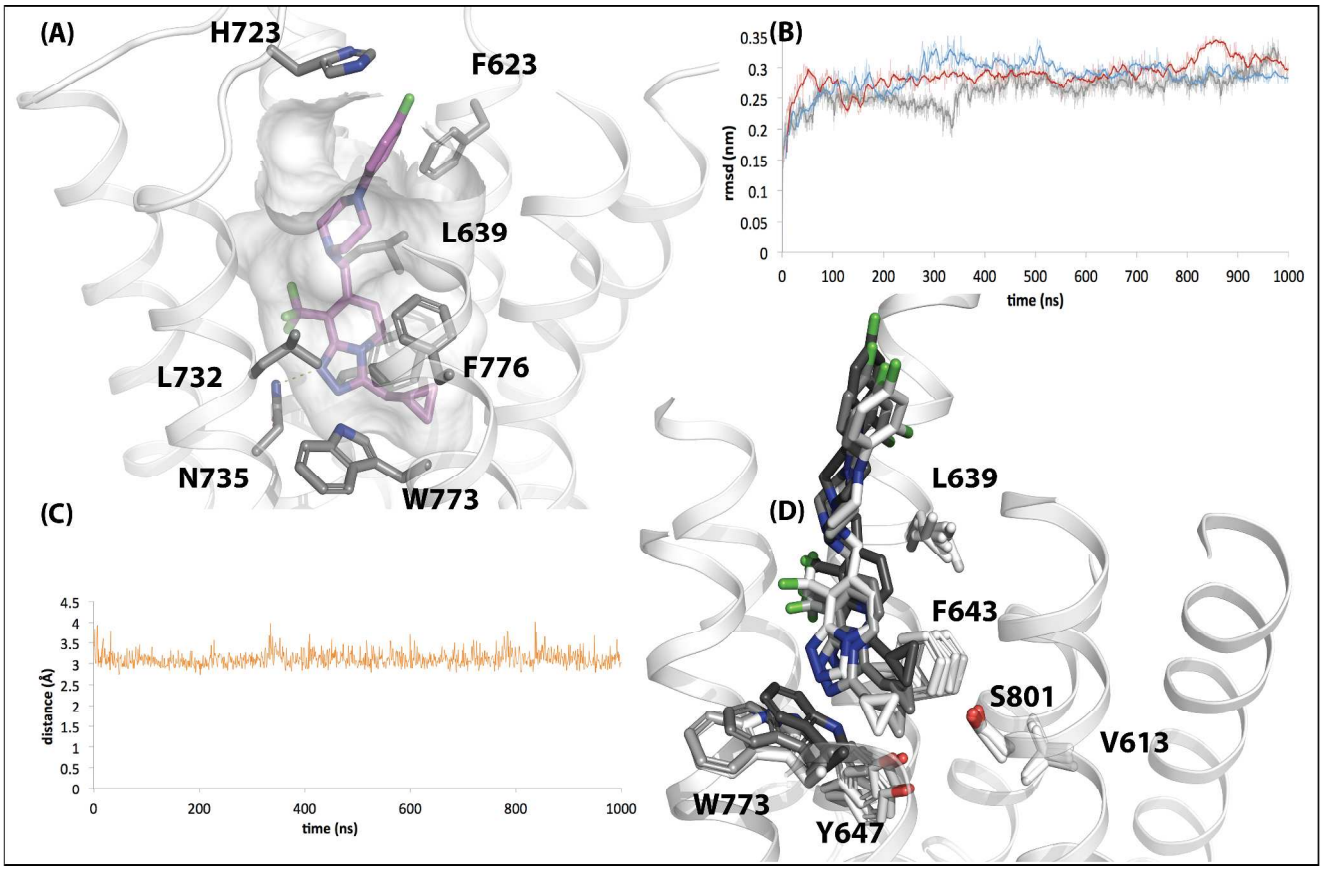

Figure 2. MD simulation of the "active" state of mGlu2 receptor in complex with the PAM **27**. (A) Proposed docking binding mode of **27** used as input for MD simulations. (B) Root-mean-square deviations (RMSD) during MD simulations on protein α-carbons after superposition of the α-carbons of the 7-transmembrane mGlu2 receptor. The three separate simulations are shown as grey, blue and red solid lines. (C) Evolution of the hydrogen bond between the nitrogen acceptor of the triazolopyridine scaffold and the amino acid N735$^{5.47a.47.c}$ (D) Snapshots of **27** and selected amino acids at different time steps of the MD simulation, showing the static nature of some sidechains compared to the inward movement of the W773$^{6.48a.50c}$.

Compound **27** was further characterized in vitro and in vivo to gain a deeper understanding of the solubility and metabolism. Thus, improved solubility in the kinetic screen was confirmed in a thermodynamic assay (Table 3) where **27** showed significantly higher solubility at pH 7.4 and more significantly at pH 2 consistent with the presence of a protonatable basic center (pK_a = 5). That improvement also may impact protein binding which, along with membrane permeability significantly decreased compared to compounds such as **5** and **6**. Moreover, the increased solubility of **27** translated into a significant improvement in several in vivo PK parameters in both rat and dog (Tables 4 and 5). Thus, **27** was rapidly absorbed and showed almost complete absorption. Unlike **5** and **6**, compound **27** showed lower clearance and longer elimination half-life after intravenous (i.v.) administration resulting in higher bioavailability and ultimately higher distribution to the brain (B/P = 2.1).

Table 3. Physico-chemical properties, permeability and rat plasma protein binding for compounds **27**, **5** and **6**.

Compd	LogP[a] / pK_a[a]	Solubility in H_2O; pH 7.4 / 2 (mg/mL)	Permeability (Caco-2 monolayers; P_{app}A->B x 10 cm s^{-1})	rat f_u plasma/brain[d] (% free)
5	4.6 / <2	<0.004 / 0.001	12[b]	0.69/0.38
6	4.4 / 4.1	<0.004 / 0.078	12[c]	0.4/0.06
27	4.2 / 5	0.05 / 2.5	22[c]	5.6/1.21

[a] Experimental values. [b] In vitro passive permeability using Caco-2 monolayers. [c] In vitro passive permeability using LLC-PK1 cells. Permeability experiments were conducted at a single concentration (1 μM) in a transwell system with an incubation of 120 min. The apical to basolateral (AtoB) transport in the presence of the P-gp inhibitor GF120918 was measured and permeation rates (Apparent Permeability) of the test compounds (Papp x10-6 cm/sec) were calculated. [d] Unbound plasma and brain concentrations determined by rapid equilibrium dialysis at a concentration of 5 μM.

Finally, **27** showed low cytochrome P450 inhibition potential for the main isoenzymes tested (3A4, 2C9, 2D6, 1A2, 2C19 and 2C8 all $IC_{50} > 20\ \mu M$) and no genotoxic potential.

Table 4. Rat PK[a] data and in vivo activity in sw-EEG for compounds **27**. **5** and **6**.

Compd	Cl (mL min/ kg)	$T_{1/2}$ (h)[b]	T_{max} (h)	$AUC_{0\text{-inf}}$ (ng.h/mL)[b]	C_{max} (ng/mL)[b]	F (%)	B/P[d]	sw-EEG LAD/LAC[e]
5	23 ± 1[b]	2.3 ± 0.5	0.5 ± 0[b]	2250 ± 417	938 ± 300	31	1	3 / 249
6	31, 37[c]	2.7 ± 0.2	0.5[c]	1804 ± 415	482 ± 151	36	1.4	3 / 65
27	16 ± 3[b]	3 ± 0.6	5 ± 3[b]	11314 ± 4286	980 ± 237	100	2.1	3 / 247

[a] Study in male Sprague-Dawley rats dosed at 10 mg/kg p.o. and 2.5 mg/kg i.v., formulated in 20% HP-β-CD + HCl solution at pH 4. [b] Values are the mean of three animals ± SD. [c] Individual values. [d] Ratios calculated after 1 h of a single dose at 10 mg/kg sc in 20% HP-β-CD + HCl solution at pH 4 in the Swiss mouse. [e] Compound administered orally. LAD stands for lowest active dose expressed in mg/kg. LAC stands for lowest active concentration in plasma, estimated on the basis of C_{max} expressed in ng/mL.

Table 5. Dog PK[a] data for compounds **27**, **5** and **6**.

Compd	Cl (mL min/kg)	$T_{1/2}$ (h)	T_{max} (h)[b]	$AUC_{0\text{-inf}}$ (ng.h/mL)	C_{max} (ng/mL)	F (%)
5	23 ± 0.8[b]	3.7 ± 0.3[b]	0.5 ± 0	743 ± 152[b]	373 ± 88[b]	20 ± 4[b]
6	29 ± 0.3[b]	1.1, 1.8[c]	0.5 ± 0	531, 957[c]	218, 472[c]	18, 33[c]
27	4, 6[c]	7, 9[c]	0.5 ± 0	3959, 9864[c]	459, 1400[c]	18, 44[c]

[a] Study in male Beagle dogs dosed at 5 mg/kg p.o. and 1 mg/kg i.v., formulated in 20% HP-β-CD + HCl solution at pH 4. [b] mean of three animals ± SD. [c] Individual values (two dogs)

In order to rule out possible off-target interactions compound **27** was tested for positive allosteric modulation, agonistic or antagonistic activity at the other mGlu receptor subtypes. **27** acts as a weak mGlu3 receptor PAM (60-fold EC_{50} ratio compared to mGlu2 PAM activity), and is >85-fold selective for mGlu2 versus other mGlu receptor subtypes. Overall, **27** showed no or negligible affinity at any of the targets in the CEREP[38] panel of receptors (>100-fold selective for mGlu2).

As in previously reported mGlu2 receptor PAM series, the in vivo pharmacological activity of compound **27** was investigated in the sleep-wake-EEG paradigm.[39] This is a highly sensitive read-out of a compound's central functional activity that may provide additional insight into its potential therapeutic application. It has been previously shown that systemic administration of an mGlu2/3 receptor agonist suppresses REM sleep in rats.[40] Internal efforts confirmed these results and have furthermore shown that this effect is mGlu2 receptor-mediated, i.e. absent in mGlu2 KO mice.[41]

After acute p.o. administration of a 3 mg/kg dose, compound **27** significantly decreased the amount of REM sleep in rats during the first 4 h without clear effects on other sleep−wake stages (see Figure 3, bottom right panel, blue bar). The active dose of 3 mg/kg p.o. corresponded to a peak of plasma concentration of 247 ng/mL, which is very comparable to those of **5** (249 ng/mL) and ~ 4-fold higher than those of **6** (65 ng/mL).

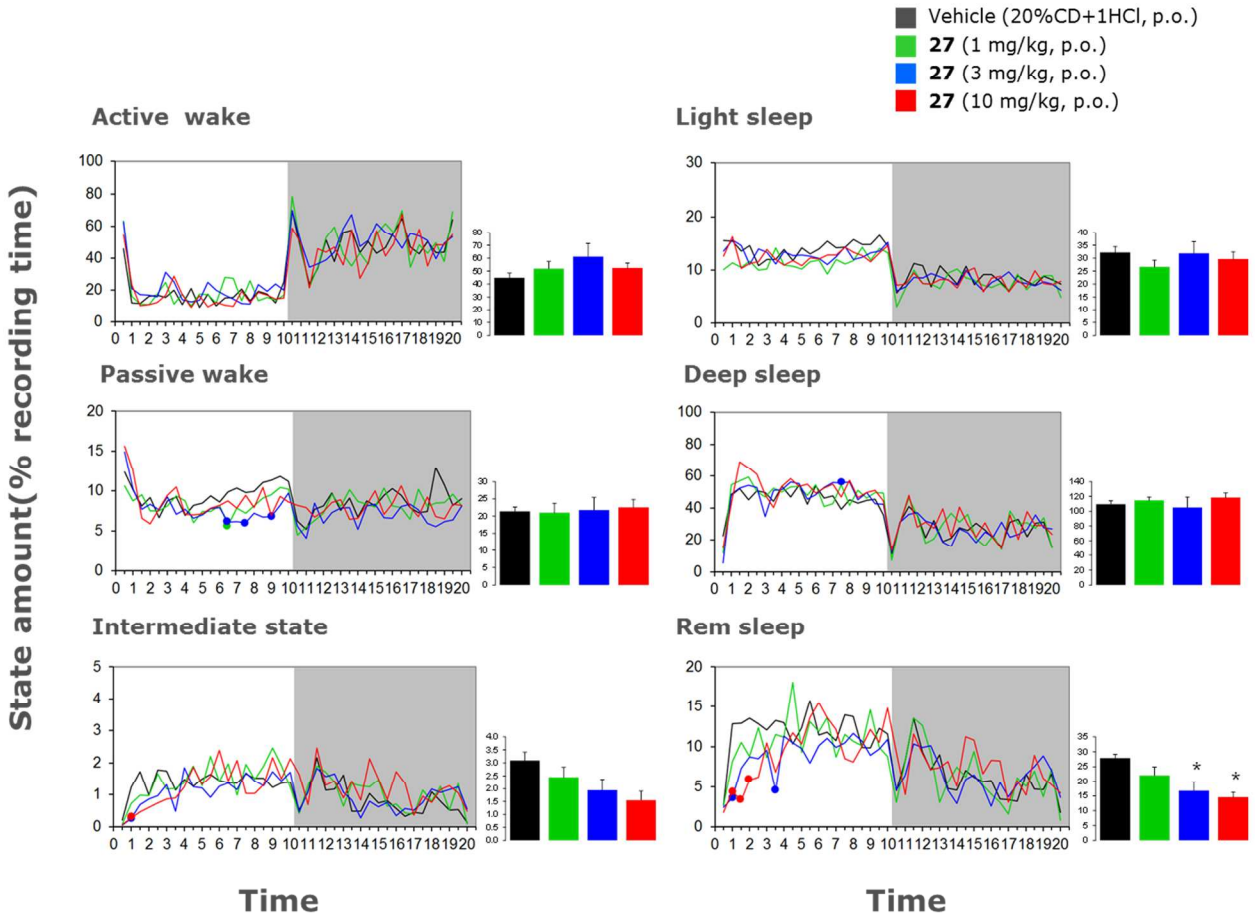

Figure 3. Effect of single oral doses of 1, 3 and 10 mg/kg of **27** or vehicle (20% CD + 1HCl) on sleep−wake organization in rats during 20 consecutive hours after administration (line graphs). Mean percentage of occurrence per 30 min period is indicated for each sleep−wake state. Shaded area indicates dark period. Small bar charts indicate average amounts of vigilance states in minutes (±SEM, n = 8 for each group) during the first 4 h post-administration. Dots on the lines of the graph indicate $p < 0.05$ versus vehicle (Wilcoxon−Mann−Whitney rank sum); * indicates $p < 0.05$: Wilcoxon−Mann−Whitney rank sum tests compared to vehicle values.

CONCLUSIONS

Herein, we report the further optimization of **6**, the most potent and selective mGlu2 PAM lead compound previously reported from our labs which had an acceptable pharmacokinetic profile in rodent and non-rodent species. Despite its promising pharmacological features, we were concerned that poor solubility and suboptimal PK could pose a challenge for achieving sufficient exposure in the clinic, thereby hindering its further development. Using **6** as a starting point, improvement of the solubility was achieved by the introduction of a methylene spacer between the piperidine ring and the triazole core. This delivered a new C-7 aminomethylene triazolopyridine class, that showed significantly increased solubility while retaining the in vitro mGlu2 PAM potency. However, that improvement turned out to be detrimental for the metabolism and hERG affinity, which was subsequently addressed by optimization of the phenylpiperidine moiety. These efforts brought us to the discovery of **27**, a compound with balanced activity vs solubility. Experimental binding, mutagenesis and computational modelling suggest that **27** shares a similar binding site and binding mode as previous leads, but with increased flexibility due to the methylene spacer. Furthermore, **27** exhibited improved drug-like properties with a better PK profile as reflected by higher oral exposures, lower clearance and higher bioavailability in rodent and non-rodent species. All this combined with improvements in central penetration and higher free

fractions positions **27** as a more suitable clinical candidate to explore a wider exposure window in eventual therapeutic indications.

Therefore, compound **27** is considered an attractive pharmacological agent to advance our knowledge of how mGlu2 receptor modulation may reduce the severity of diseases where disruption of glutamatergic transmission is pronounced.

ASSOCIATED CONTENT

Biology. Membrane Preparation. CHO cells expressing the human mGlu2 receptor were grown until they were 80% confluent, washed in ice-cold phosphate buffered saline, and stored at −20 °C until membrane preparation. After thawing, cells were suspended in 50 mM Tris-HCl, pH 7.4, and collected through centrifugation for 10 min at 23 500g at 4 °C. Cells were lysed in 5 mM hypotonic Tris-HCl, pH 7.4, and after recentrifugation for 20 min at 30 000g at 4 °C, the pellet was homogenized with an Ultra Turrax homogenizer in 50 mM Tris- HCl, pH 7.4. Protein concentrations were measured by the Bio-Rad protein assay using bovine serum albumin as standard.

[^{35}S]GTPγS Binding Assay. For [^{35}S]GTPγS measurements, compound and glutamate were diluted in buffer containing 10 mM HEPES acid, 10 mM HEPES salt, pH 7.4, containing 100 mM NaCl, 3 mM $MgCl_2$, and 10 μM GDP. Membranes were thawed on ice and diluted in the same buffer, supplemented with 14 μg/mL saponin (final assay concentration of 2 μg/mL saponin). Final assay mixtures contained 7 μg of membrane protein and were preincubated with compound alone (determination of agonist effects) or together with an EC_{20} concentration (4 μM) of glutamate (determination of PAM effects) for 30 min at 30 °C. [^{35}S]GTPγS was added at a final concentration of 0.1 nM and incubated for another 30 min at 30 °C. Reactions were terminated by rapid filtration through Unifilter-96 GF/ B filter plates (Packard) using a 96-well Packard filtermate harvester. Filters were washed six times with ice-cold 10 mM NaH_2PO_4/10 mM Na_2HPO_4, pH 7.4, and filter-bound radioactivity was counted in a microplate scintillation and luminescence counter from Packard.

Data Analysis. Data were processed using an internal software interface and were calculated as the percent of the control agonist challenge. Sigmoid concentration−response curves plotting these percentages versus the log concentration of the test compound were analyzed using nonlinear regression analysis. The EC_{50} is the concentration of a compound that causes a half-maximal potentiation of the glutamate response. The pEC_{50} values are calculated as the –log EC_{50} (wherein EC_{50} is expressed in mol L−1).

Sleep−Wake EEG: Animals, Drug Treatment, and Experimental Procedure. All in vivo experimental procedures were performed according to the applicable European Communities Council Directive of November 24, 1986 (86/609/EEC) and approved by the Animal Care and Use Committee of Janssen Pharmaceutical Companies of Johnson & Johnson and by the local ethical committee. Male Sprague−Dawley rats (Charles River, France) weighing 250−300 g were used. Animals were chronically implanted with electrodes for recording the cortical electroencephalogram (EEG), electrical neck muscle activity (EMG), and ocular movements (EOG). All animals were housed in individually ventilated cages under environmentally controlled conditions (ambient temperature, 22 °C; humidity, 60%) on a 12 h light/dark cycle (lights on from 12:00 a.m. to 12:00 p.m., illumination intensity of ∼100 lx). The animals had free access to food and tap water. The effects of the tested molecule and vehicle on sleep−wake distribution during the lights-on period were investigated in 16 rats (n = 8 each group). Two EEG recording sessions were performed: the first recording session started at 13:30 h and lasted 20 h following oral administration of saline. The second recording session was performed during the same consecutive circadian time and for the same duration following administration of either vehicle (20% CD + $2H_2T$) or tested compound. Sleep polysomnographic variables were determined offline as described elsewhere using a sleep stages analyzer, scoring each 2 s epoch before averaging stages over 30 min periods. Sleep−wake state classifications were assigned on the basis of the combination of dynamics of five EEG frequency domains, integrated EMG, EOG, and body activity level: active wake (AW); passive wake (PW); intermediate stage (pre-REM transients); rapid eye movement sleep (REM); light non-REM sleep (lSWS); deep non-REM sleep (dSWS). Different sleep−wake parameters were

investigated over 20 h post-administration, and time spent in each vigilance state, sleep parameters, latencies for first REM sleep period and the number of transitions between states were determined.

Statistical Analysis. Time spent in each vigilance state (AW, PW, lSWS, dSWS, IS, and REMS) was expressed as a percentage of the recording period. A statistical analysis of the obtained data was carried out by a nonparametric analysis of variance of each 30 min period, followed by a Wilcoxon−Mann−Whitney rank sum test of comparisons with the control group.

Mutagenesis experiments. The methodology is identical to as described in the work of Farinha et al.[36] In brief, cDNA encoding human non-mutated and mutated mGlu2 receptors was synthesized by GeneArt® (Life Technologies, Carlsbad, CA, USA) and subcloned to the mammalian expression vector pcDNA3.1(+) (Life Technologies). Plasmid DNA was amplified through Escherichia coli transformation and used for transient transfection in CHO-K1 cells. All transfections were performed using the cationic lipid transfection reagent Lipofectamine™ (Life Technologies). The cells were maintained in DMEM supplemented with 10% heat-inactivated FBS, penicillin G, streptomycin sulphate, pyruvic acid and L-glutamine. Cells were washed, thawed and treated as described above for membrane preparation. Also, the [^{35}S]GTPγS assay was performed as described above. Proper mutant receptor expression and glutamate agonistic activity was previously tested.[36]

Data Analysis. The concentration−response curves in the presence of added EC_{25} of mGlu2 agonist glutamate to determine positive allosteric modulation (PAM) were generated using the Prism GraphPad software (Graph Pad Inc., San Diego, CA, U.S.). The curves were fitted to a four-parameter logistic equation Y = Bottom + (Top − Bottom)/(1 + 10(log EC_{50}−X)Hill slope) allowing determination of EC_{50} values. The EC_{50} is the concentration of a compound that causes a half-maximal potentiation of the glutamate response. This is calculated by subtracting the maximal responses of glutamate in the presence of a fully saturating concentration of a positive allosteric modulator from the response of glutamate in the absence of a positive allosteric modulator. The concentration producing the half-maximal effect is then calculated as EC_{50}. The pEC_{50} values are calculated as the −log EC_{50} (wherein EC_{50} is expressed in mol L^{-1}).

Molecular modeling. An active state mGlu2 receptor model was built into which the compound was docked using GlideXP and the best binding pose was subjected to molecular dynamics simulations. The mGlu2 receptor model was built using a combination of structural templates. The 7-transmembrane and loop sections of the human mGlu2 receptor (Uniprot code Q14416) model were based on the crystal structures of the human mGlu5 receptor (PDB ID 4OO9)[42] and mGlu1 receptor (PDB ID 4OR2)[43]. To account for the open conformation of transmembrane helix 6 which is expected in an active state conformation, this helix was modelled based on the active structure of the β_2AR (PDB ID 3SN6)[44]. The structure was prepared for further work within Maestro[45], for instance to fix missing sidechains/atoms, assigning protein protonation states with PROPKA, optimize the hydrogen bonding network, etc. The ligand was prepared for docking using the LigPrep tool and conformers of **27** were calculated with ConfGen. The 3D conformers were docked into the receptor model using Glide XP with the grid centered on the crystallized ligand in the mGlu1 receptor. The Glide XP scoring function was used, and sampling was increased through modifying a number of parameters within Glide: expanded sampling was turned on, and 100 initial poses were passed to post-docking minimisation. All other docking parameters were set to the defaults. Docking solutions were then visually inspected.

Molecular dynamics simulations were performed with the GROMACS v 5.0.5 simulation package.[46] The ligand-receptor complexes were embedded in a pre-equilibrated box (10x10x19 nm) containing a lipid bilayer (297 molecules of POPC) with explicit solvent (~47.000 water) and 0.15 M concentration of Na+ and Cl- (~490 ions).[47] The model system was energy minimized and subsequently subjected to a 5 steps MD equilibration. The first step was a 10ns equilibration with the whole system fixed except hydrogens. Then a 5 ns equilibration was performed in which the loops of the protein were released from restraints, using the dssp program[48] to calculate secondary structure. Finally, three steps of 2 ns each were performed, the restraints in the ligand and the protein were consecutively relaxed (100-50-10 Kcal). After these restraints were released, the final 1000 ns production simulation was performed. An additional two replicas of 1000 ns were also performed using different initial velocities. All simulations were run at a constant temperature of 300 K using separate v-rescale thermostats for Protein-Ligand,

lipid and water and ions.[49] A time step of 2fs was used for the integration of equation of motion. All bonds and angles were kept frozen using LINCS algorithm.[50] Lennard-Jones interactions were computed using a cutoff of 10 Å, and the electrostatic interactions were treated using PME[51] with the same real-space cutoff. The AMBER99SD-ILDN force field[52] was used for the protein, the parameters described by Berger and co-workers for lipids,[53] and the general Amber force field (GAFF) and HF/6-31G*-derived RESP atomic charges for the ligand.[54] This combination of protein and lipid parameters has recently been validated.[55]

Patch-Clamp Assay. Experiments were performed using HEK293 cells stably expressing the hERG potassium channel. Cells were grown at 37 °C and 5% CO2 in culture flasks in MEM medium supplemented with 10% heat-inactivated fetal bovine serum, 1% L-glutamine− penicillin−streptomycin solution, 1% nonessential amino acids (100×), 1% sodium pyruvate (100 mM), and 0.8% Geneticin (50 mg/mL). Before use, the cells were subcultured in MEM medium in the absence of 5 mL of L-glutamine−penicillin−streptomycin. For use in the automated patch-clamp system PatchXpress 7000A (Axon Instruments), cells were harvested to obtain cell suspension of single cells. The extracellular solution contained the following (mM): 150 NaCl, 4 KCl, 1 $MgCl_2$, 1.8 $CaCl_2$, 10 HEPES, 5 glucose (pH 7.4 with NaOH). The pipette solution contained the following (mM): 120 KCl, 10 HEPES, 5 EGTA, 4 ATP-Mg^{2+}, 2 $MgCl_2$, 0.5 $CaCl_2$ (pH 7.2 with KOH). Patch-clamp experiments were performed in the voltage clamp mode, and whole-cell currents were recorded with an automated patch-clamp assay utilizing the PatchXpress 7000A system (Axon Instruments). Current signals were amplified and digitized by a multiclamp amplifier, stored, and analyzed by using the PatchXpress and DataXpress software and Igor 5.0 (Wavemetrics). The holding potential was −80 mV. The hERG current (K+-selective outward current) was determined as the maximal tail current at −40 mV after a 2 s depolarization to +60 mV. The pulse cycling rate was 15 s. Before each test pulse, a short pulse (0.5 s) from the holding potential to −60 mV was given to determine (linear) leak current. After establishment of whole-cell configuration and a stability period, the vehicle was applied for 5 min followed by the test substance at increasing concentrations of 10^{-7}, 3×10^{-7}, and 3×10^{-6} M. Each concentration of the test

substance was applied twice. The effect of each concentration was determined after 5 min as an average current of three sequential voltage pulses. To determine the extent of block, the residual current was compared with vehicle pretreatment.

Chemistry. Unless otherwise noted, all reagents and solvents were obtained from commercial suppliers and used without further purification. Thin layer chromatography (TLC) was carried out on silica gel 60 F254 plates (Merck). Flash column chromatography was performed on silica gel, particle size 60 Å, mesh of 230−400 (Merck) under standard techniques. Microwave assisted reactions were performed in a single-mode reactor, Biotage Initiator Sixty microwave reactor (Biotage), or in a multimode reactor, MicroSYNTH Labstation (Milestone, Inc.). Nuclear magnetic resonance (NMR) spectra were recorded with either a Bruker DPX-400 or a Bruker AV-500 spectrometer (Bruker AG) with standard pulse sequences, operating at 400 and 500 MHz, respectively, using $CDCl_3$ and DMSO-d_6 as solvents. Chemical shifts (δ) are reported in parts per million (ppm) downfield from tetramethylsilane (δ = 0). Coupling constants are reported in hertz. Splitting patterns are defined by s (singlet), d (doublet), dd (double doublet), t (triplet), q (quartet), quin (quintet), sex (sextet), sep (septet), or m (multiplet).

Liquid chromatography combined with mass spectrometry (LCMS) was performed using either an HP 1100 HPLC system (Agilent Technologies, Waldbronn, Germany) or an Acquity UPLC® system (Waters®, Milford, MA, USA) comprising an LC pump (quaternary or binary) with degasser, an autosampler, a column oven, a diode array detector (DAD), and a column as specified in the respective methods. Flow from the column was brought to the MS spectrometer. The MS detector (either SQD or TOF) was configured with an atmospheric pressure ion source. Nitrogen was used as the nebulizer gas. Data acquisition was performed with MassLynx-Openlynx software or with Chemsation-Agilent data browser software. More detailed information about the different LCMS methods employed can be found in the Supporting Information. Melting point values are peak values and were obtained with experimental uncertainties that are commonly associated with this analytical method. Melting points

were determined in open capillary tubes either on a Mettler FP62 (A) or a Mettler FP 81HT / FP90 (B) apparatus with a temperature gradient of 10 °C/min. Maximum temperature was 300 °C.

Purities of all new compounds were determined by analytical reverse phase RP HPLC or RP UPLC coupled to a mass spectrometry detector, using the area percentage method on the UV trace scanning from 200 to 450 nm, and compounds were found to have ≥95% purity unless otherwise specified.

7-Vinyl-3-cyclopropylmethyl-8-trifluoromethyl[1,2,4]triazolo[4,3-a]pyridine (8). A suspension of **7** (1.65 g, 5.986 mmol), vinylboronic acid pinacol ester (1.218 ml, 7.183 mmol), $Pd(PPh_3)_4$ (0.346, 0.3 mmol) and $NaHCO_3$ (aqueous sat. solution, 12.5 mL) in 1,4-dioxane (64.5 mL) was heated at 150 ºC under microwave irradiation for 13 min. After cooling, the resulting reaction mixture was diluted with EtOAc/water and filtered through a pad of diatomaceous earth. The filtrate was washed with water and NaCl (aqueous sat. solution) and extracted with EtOAc. The organic layer was separated, dried (Na_2SO_4) and concentrated *in vacuo*. The residue was purified again by column chromatography (silica; EtOAc in DCM 0/100 to 40/60). The desired fractions were collected and concentrated *in vacuo* to give **8** (1.34 g, 83.7%). LCMS: *m/z* 268 $[M + H]^+$, t_R = 2.27 min. ^{1}H NMR (500 MHz, $CDCl_3$) δ ppm 0.29 - 0.40 (m, 2 H), 0.57 - 0.69 (m, 2 H), 1.14 - 1.23 (m, 1 H), 3.10 (d, *J*=6.6 Hz, 2 H), 5.72 (d, *J*=11.0 Hz, 1 H), 5.94 (d, *J*=17.3 Hz, 1 H), 7.09 (d, *J*=7.2 Hz, 1 H), 7.18 - 7.28 (m, 1 H), 8.07 (d, *J*=7.2 Hz, 1 H)

7-Carboxaldehyde-3-cyclopropylmethyl-8-trifluoromethyl[1,2,4]triazolo[4,3-a]pyridine (9). A solution of **8** (6.24 g, 21.014 mmol), sodium periodate (13.484 g, 63.041 mmol), osmium tetroxide (2.5% in tert-butanol, 10.873 mL, 0.841 mmol) in water (55 mL) and 1,4-dioxane (221 mL) was stirred at rt for 2 h. The resulting reaction mixture was diluted with EtOAc/water and filtered through a pad of diatomaceous earth. The filtrate was extracted with EtOAc. The organic layer was separated, dried (Na_2SO_4) and concentrated *in vacuo*. The solid residue was washed with Et_2O, filtered and dried *in vacuo* to give **9** (3.84 g, 67.9%). LCMS: *m/z* 270 $[M + H]^+$, t_R = 1.62 min. ^{1}H NMR (500 MHz, $CDCl_3$) δ ppm 0.32 - 0.43 (m, 2 H), 0.61 - 0.73 (m, 2 H), 1.16 - 1.29 (m, 1 H), 3.17 (d, *J*=6.9 Hz, 2 H), 7.49 (d, *J*=7.2 Hz, 1 H), 8.21 (d, *J*=7.2 Hz, 1 H), 10.54 (d, *J*=1.2 Hz, 1 H).

7-Hydroxymethyl-3-cyclopropylmethyl-8-trifluoromethyl[1,2,4]triazolo[4,3-a]pyridine (10). To a solution of **9** (1.73 g, 6.426 mmol) in MeOH (58 mL) stirred at 0º C, was added portionwise sodium borohydride (0.243, 6.426 mmol). The resulting mixture was stirred at rt for 1 h. The resulting mixture was concentrated *in vacuo*. The residue was treated with water and NaCl (aqueous sat. solution) and extracted with EtOAc. The organic layer was separated and concentrated *in vacuo*. The residue was purified by column chromatography (silica; MeOH/NH_3 in DCM 0/100 to 5/95). The desired fractions were collected and concentrated *in vacuo* to give **10** (1.015 g, 58%) as a brown syrup. LCMS: *m/z* 272 $[M + H]^+$, t_R = 0.53 min. ^{1}H NMR (400 MHz, $CDCl_3$) δ ppm 0.15 - 0.36 (m, 2 H), 0.46 - 0.64 (m, 2 H), 1.04 - 1.19 (m, 1 H), 3.01 (d, *J*=6.7 Hz, 2 H), 5.00 (br s, 2 H), 6.26 (br s, 1 H), 7.63 (d, *J*=7.2 Hz, 1 H) 8.12 (d, *J*=7.4 Hz, 1 H).

7-(Methylsulfonyloxy)methyl-3-cyclopropylmethyl-8-trifluoromethyl[1,2,4]triazolo[4,3-a]pyridine (11). To a solution of **10** (1.341 g, 9.678 mmol) and Et_3N (0.778 mL, 5.612 mmol) in DCM (42 mL) stirred at 0ºC, was added dropwise methylsulfonyl chloride (0.749 mL, 9.678 mmol) and stirred at rt for 2 h. The resulting mixture was treated with $NaHCO_3$ (aqueous sat. solution) and extracted with DCM. The organic layer was separated and concentrated *in vacuo* to give **11** (2.6 g, 87%). LCMS: *m/z* 350 $[M + H]^+$, t_R = 0.74 min. ^{1}H NMR (400 MHz, $CDCl_3$) δ ppm 0.28 - 0.41 (m, 2 H), 0.57 - 0.70 (m, 2 H), 1.14 - 1.25 (m, 1 H), 3.13 (d, *J*=6.7 Hz, 2 H), 3.16 (s, 3 H), 5.49 (br d, *J*=1.6 Hz, 2 H), 7.17 (d, *J*=7.2 Hz, 1 H), 8.30 (d, *J*=7.2 Hz, 1 H).

8-Trifluoromethyl-3-cyclopropylmethyl-7-[(4-phenyl-1-piperidinyl)methyl]-1,2,4-triazolo[4,3-a]pyridine (12). 5 (0.4 g, 0.9 mmol) was added to a stirred solution of phenylpiperidine (0.174 mg, 1.08 mmol) and DIPEA (0.233 mL, 1.35 mmol) in CH_3CN (10 mL). The resulting mixture was heated in a sealed tube at 100 ºC for 4 h. The resulting mixture was concentrated *in vacuo*. The residue was purified by column chromatography (silica gel; DCM/EtOAc from 100/0 to 50/50 as eluent). The desired fractions were collected and concentrated *in vacuo*. The residue thus obtained was triturated with DIPE to yield final compound **12** (0.272 g, 77%) as a white solid. LCMS: *m/z* 415 $[M + H]^+$, t_R = 3.46 min.

^{1}H NMR (500 MHz, DMSO-d_6) δ ppm 0.27 - 0.40 (m, 1 H), 0.45 - 0.62 (m, 2 H), 1.14 - 1.34 (m, 1 H), 1.94 (br. d, *J*=13.3 Hz, 2 H), 2.15 - 2.34 (m, 2 H), 2.81 - 2.95 (m, 1 H), 3.12 (d, *J*=6.9 Hz, 2 H), 3.16 - 3.33 (m, 2 H), 3.54 (br. d, *J*=11.6 Hz, 2 H), 4.61 (br. s., 2 H), 7.17 - 7.29 (m, 3 H), 7.34 (t, *J*=7.5 Hz, 2 H), 7.88 (d, *J*=7.2 Hz, 1 H), 8.93 (d, *J*=7.2 Hz, 1 H), 11.22 (br. s., 1 H). M. p. 144.6 ºC (B).

8-Trifluoromethyl-3-cyclopropylmethyl-7-[(4-phenyl-4-fluoro-1-piperidinyl)methyl]-1,2,4-triazolo[4,3-a]pyridine (13). To a solution of 4-fluoro-4-phenylpiperidine hydrochloride [C.A.S. 1056382-25-2] (0.096 g, 0.446 mmol) in DCE stirred at rt (2.14 mL) was added **3** (0.1 g, 0.371 mmol) and the resulting mixture was stirred at rt overnight. Then, acetic acid (0.037 mL) was added and stirred at rt for 4 h. Then, sodium triacetoxy-borohydride (0.87 g, 0.409 mmol) was added and stirred at rt overnight. The reaction mixture was neutralized with Na_2CO_3 (aqueous sat. solution) and extracted with DCM. The organic layer was dried (Na_2SO_4) and concentrated *in vacuo*. The crude product thus obtained was purified by column chromatography (silica gel; DCM/EtOAc from 100/0 to 50/50 as eluent). The desired fractions were collected and concentrated *in vacuo*. The residue obtained was triturated with Et_2O to give **13** (0.029 g, 18%). LCMS: *m/z* 433 $[M + H]^+$, t_R = 3.26 min. ^{1}H NMR (500 MHz, $CDCl_3$) δ ppm 0.31 - 0.41 (m, 2 H), 0.59 - 0.69 (m, 2 H), 1.14 - 1.24 (m, 1 H), 2.02 (br t, *J*=11.7 Hz, 2 H), 2.05 - 2.13 (m, 1 H), 2.17 (td, *J*=13.2, 4.8 Hz, 1 H), 2.65 (br t, *J*=11.0 Hz, 2 H), 2.71 - 2.81 (m, 2 H), 3.11 (d, *J*=6.9 Hz, 2 H), 3.82 (d, *J*=1.4 Hz, 2 H), 7.29 - 7.34 (m, 1 H), 7.36 - 7.46 (m, 4 H), 7.39 (d, *J*=7.2 Hz, 1 H), 8.06 (d, *J*=7.2 Hz, 1 H). M. p. 179.2 °C (B).

8-Trifluoromethyl-3-cyclopropylmethyl-7-[(4-phenyl-4-trifluoromethyl-1-piperidinyl)methyl]-1,2,4-triazolo[4,3-a]pyridine (14). Starting from **9** (0.1 g, 0.371 mmol) and 4-trifluoro-4-phenylpiperidine hydrochloride [C.A.S. 1254981-45-7] (0.102 g, 0.446 mmol) and following the procedure described for **13**, compound **14** was obtained as a solid (0.073 g, 39%). LCMS: *m/z* 483 $[M + H]^+$, t_R = 2.75 min. ^{1}H NMR (500 MHz, $CDCl_3$) δ ppm 0.30 - 0.41 (m, 2 H), 0.59 - 0.70 (m, 2 H), 1.15 - 1.24 (m, 1 H), 2.14 - 2.28 (m, 4 H), 2.67 - 2.77 (m, 1 H), 3.10 (d, *J*=6.6 Hz, 2 H), 3.60 (br s, 2 H), 7.34 - 7.42 (m, 2 H), 7.42 - 7.47 (m, 4 H), 8.05 (d, *J*=7.2 Hz, 1 H). M. p. 128.0 °C (B).

8-Trifluoromethyl-3-cyclopropylmethyl-7-[(4-phenyl-4-methoxy-1-piperidinyl)methyl]-1,2,4-triazolo[4,3-a]pyridine (15). Starting from **11** (0.4 g, 0.9 mmol) and 4-methoxy-4-phenylpiperidine hydrochloride [C.A.S. 83949-38-6] (0.072 mg, 0.378 mmol) and following the procedure described for **12**, compound **15** was obtained as a white solid (0.084 g, 60%). LCMS: *m/z* 445 $[M + H]^+$, t_R = 3.16 min. ^{1}H NMR (400 MHz, $CDCl_3$) δ ppm 0.28 - 0.41 (m, 2 H), 0.56 - 0.70 (m, 2 H), 1.15 - 1.23 (m, 1 H), 1.59 (br s, 1 H) 1.92 - 2.11 (m, 4 H), 2.55 - 2.71 (m, 4 H), 2.97 (s, 3 H), 3.10 (d, *J*=6.7 Hz, 2 H), 3.79 (d, *J*=1.6 Hz, 2 H), 7.27 - 7.32 (m, 1 H), 7.33 - 7.43 (m, 4 H), 7.44 (d, *J*=7.4 Hz, 1 H), 8.04 (d, *J*=7.2 Hz, 1 H). M. p. 143.1 °C (B).

3-(Cyclopropylmethyl)-7-[(3-phenyl-1-piperidinyl)methyl]-8-(trifluoromethyl)-1,2,4-triazolo[4,3-a]pyridine (16). Starting from **11** (0.123 g, 0.315 mmol) and 3-phenylpiperidine (0.063 g, 0.394 mmol), and following the procedure described for **12**, compound **16** was obtained as a white solid (0.011 g, 9%). LCMS: *m/z* 415 $[M + H]^+$, t_R = 3.45 min. ^{1}H NMR (500 MHz, $CDCl_3$) δ ppm 0.29 - 0.40 (m, 2 H), 0.58 - 0.69 (m, 2 H), 1.14 - 1.24 (m, 1 H), 1.50 (qd, *J*=12.5, 4.2 Hz, 1 H), 1.69 - 1.77 (m, 1 H), 1.78 - 1.86 (m, 1 H), 1.91 - 2.02 (m, 1 H), 2.18 (td, *J*=11.5, 2.7 Hz, 1 H), 2.24 (t, *J*=11.0 Hz, 1 H), 2.77 - 2.87 (m, 2 H), 2.88 - 2.95 (m, 1 H), 3.09 (d, *J*=6.6 Hz, 2 H), 3.68 - 3.84 (m, 2 H), 7.16 - 7.24 (m, 3 H), 7.27 - 7.33 (m, 2 H), 7.46 (d, *J*=7.2 Hz, 1 H), 8.05 (d, *J*=7.2 Hz, 1 H).

3-(Cyclopropylmethyl)-7-[(3-methyl-3-phenyl-1-piperidinyl)methyl]-8-(trifluoromethyl)-1,2,4-triazolo[4,3-a]pyridine (17). Starting from **9** (0.085 g, 0.316 mmol) and (*RS*)-3-methyl-3-phenylpiperidine [(C.A.S. 19735-13-8), 0.075 g, 0.428 mmol] and following the procedure described for **13**, compound **17** was obtained as a white solid (0.07 g, 45.5 %). LCMS: *m/z* 429 $[M + H]^+$, t_R = 3.45 min. ^{1}H NMR (400 MHz, $CDCl_3$) δ ppm 0.29 - 0.41 (m, 2 H), 0.57 - 0.70 (m, 2 H), 1.14 - 1.22 (m, 1 H), 1.22 - 1.27 (m, 1 H), 1.30 (br. s, 3 H), 1.53 - 1.62 (m, 1 H), 1.67 - 1.82 (m, 1 H), 1.88 - 2.06 (m, 1 H), 2.32 - 2.45 (m, 1 H), 2.51 (br. d, *J*=10.9 Hz, 2 H), 2.78 (br. d, *J*=9.7 Hz, 1 H), 3.03 - 3.16 (m, 2 H), 3.67 - 3.80 (m, 2 H), 7.16 - 7.24 (m, 1 H), 7.27 - 7.40 (m, 5 H), 8.00 (d, *J*=7.4 Hz, 1 H). M. p. 148.5 °C (A).

8-Trifluoromethyl-3-cyclopropylmethyl-7-[(4-(2-fluorophenyl)-1-piperidinyl)methyl]-1,2,4-triazolo[4,3-a]pyridine (18). Starting from **5** (0.140 g, 0.315 mmol) and 4-(2-fluorophenyl)piperidine (0.075 g, 0.378 mmol), and following the procedure described for **12**, compound **18** was obtained (0.065 g, 49%). LCMS: *m/z* 433 $[M + H]^+$, t_R = 3.49 min. ^{1}H NMR (500 MHz, $CDCl_3$) δ ppm 0.30 - 0.41 (m, 2 H), 0.58 - 0.69 (m, 2 H), 1.15 - 1.24 (m, 1 H), 1.75 - 1.90 (m, 4 H), 2.26 - 2.36 (m, 2 H), 2.84 - 2.99 (m, 3 H), 3.10 (d, *J*=6.6 Hz, 2 H), 3.77 (d, *J*=1.4 Hz, 2 H), 6.97 - 7.06 (m, 1 H), 7.07 - 7.14 (m, 1 H), 7.15 - 7.22 (m, 1 H), 7.22 - 7.27 (m, 1 H), 7.47 (d, *J*=7.2 Hz, 1 H), 8.06 (d, *J*=7.2 Hz, 1 H). M. p. 151 °C (B).

8-Trifluoromethyl-3-cyclopropylmethyl-7-[(4-(2-chlorophenyl)-1-piperidinyl)methyl]-1,2,4-triazolo[4,3-a]pyridine (19). Starting from **11** (0.140 g, 0.315 mmol) and 4-(2-chlorophenyl)piperidine (0.087 g, 0.378 mmol), and following the procedure described for **12**, compound **19** was obtained as a white solid (0.041 g, 29%). LCMS: *m/z* 449 $[M + H]^+$, t_R = 3.76 min. ^{1}H NMR (500 MHz, $CDCl_3$) δ ppm 0.31 - 0.40 (m, 2 H), 0.58 - 0.69 (m, 2 H), 1.15 - 1.24 (m, 1 H), 1.74 (qd, *J*=12.1, 3.2 Hz, 2 H), 1.88 (br d, *J*=12.7 Hz, 2 H), 2.34 (td, *J*=11.8, 2.0 Hz, 2 H), 2.94 (br d, *J*=11.6 Hz, 2 H), 3.07 (tt, *J*=12.1, 3.5 Hz, 1 H), 3.10 (d, *J*=6.6 Hz, 2 H), 3.78 (br d, *J*=1.7 Hz, 2 H), 7.15 (td, *J*=7.8, 1.7 Hz, 1 H), 7.23 (dd, *J*=8.1, 0.9 Hz, 1 H), 7.29 (dd, *J*=7.8, 1.7 Hz, 1 H), 7.36 (dd, *J*=8.1, 1.2 Hz, 1 H), 7.46 (d, *J*=7.5 Hz, 1 H), 8.05 (d, *J*=7.2 Hz, 1 H).

8-Trifluoromethyl-3-cyclopropylmethyl-7-[(4-(2,6-difluorophenyl)-1-piperidinyl)methyl]-1,2,4-triazolo[4,3-a]pyridine (20). Starting from **11** (0.123 g, 0.316 mmol) and 4-(2,6-difluorophenyl)piperidine (0.097 g, 0.395 mmol), and following the procedure described for **12**, compound **20** was obtained as a white solid (0.049 g, 35%). LCMS: *m/z* 451 $[M + H]^+$, t_R = 3.55 min. ^{1}H NMR (500 MHz, $CDCl_3$) δ ppm 0.30 - 0.41 (m, 2 H), 0.58 - 0.70 (m, 2 H), 1.14 - 1.24 (m, 1 H), 1.72 (br d, *J*=13.3 Hz, 2 H), 2.12 - 2.23 (m, 2 H), 2.23 - 2.32 (m, 2 H), 2.91 (br d, *J*=11.0 Hz, 2 H), 3.03 (tt, *J*=12.1, 3.5 Hz, 1 H), 3.11 (d, *J*=6.9 Hz, 2 H), 3.77 (d, *J*=1.4 Hz, 2 H), 6.84 (t, *J*=8.2 Hz, 2 H), 7.09 - 7.18 (m, 1 H), 7.53 (d, *J*=7.2 Hz, 1 H), 8.07 (d, *J*=7.2 Hz, 1 H). M. p. 186.2 °C (B).

8-Trifluoromethyl-3-cyclopropylmethyl-7-[(4-(2,4-difluorophenyl)-1-piperidinyl)methyl]-1,2,4-triazolo[4,3-a]pyridine (21). Starting from **9** (0.1 g, 0.371 mmol) and 4-(2,4-difluorophenyl)piperidine [C.A.S. 291289-50-4] (0.088 g, 0.446 mmol) and following the procedure described for **13**, compound **21** was obtained (0.099 g, 59%). LCMS: *m/z* 451 $[M + H]^+$, t_R = 3.58 min. ^{1}H NMR (500 MHz, $CDCl_3$) δ ppm 0.30 - 0.41 (m, 2 H), 0.58 - 0.69 (m, 2 H), 1.15 - 1.24 (m, 1 H), 1.72 - 1.87 (m, 4 H), 2.30 (td, *J*=11.6, 2.9 Hz, 2 H), 2.80 - 2.89 (m, 1 H), 2.92 (br d, *J*=11.6 Hz, 2 H), 3.10 (d, *J*=6.6 Hz, 2 H), 3.77 (d, *J*=1.7 Hz, 2 H), 6.78 (ddd, *J*=11.0, 9.0, 2.3 Hz, 1 H), 6.83 (td, *J*=8.2, 2.0 Hz, 1 H), 7.16 - 7.22 (m, 1 H), 7.45 (d, *J*=7.2 Hz, 1 H), 8.06 (d, *J*=7.2 Hz, 1 H). M. p. 153.4 °C (B).

8-Trifluoromethyl-3-cyclopropylmethyl-7-[(4-(2,4-difluorophenoxy)-1-piperidinyl)methyl]-1,2,4-triazolo[4,3-a]pyridine (22). Starting from **11** (0.140 g, 0.315 mmol) and 4-(2,4-difluorophenoxy)piperidine [C.A.S. 367501-08-4] (0.081 g, 0.378 mmol), and following the procedure described for **12**, compound **22** was obtained as a white solid (0.009 g, 6%). LCMS: *m/z* 467 $[M + H]^+$, t_R = 3.28 min. ^{1}H NMR (400 MHz, $CDCl_3$) δ ppm 0.29 - 0.41 (m, 2 H), 0.57 - 0.70 (m, 2 H), 1.14 - 1.25 (m, 1 H), 1.79 - 1.91 (m, 2 H), 1.94 - 2.05 (m, 2 H), 2.30 - 2.41 (m, 2 H), 2.74 - 2.83 (m, 2 H), 3.10 (d, *J*=6.7 Hz, 2 H), 3.75 (br d, *J*=1.6 Hz, 2 H), 4.18 - 4.27 (m, 1 H), 6.74 - 6.82 (m, 1 H), 6.82 - 6.90 (m, 1 H), 6.92 - 7.01 (m, 1 H), 7.42 (d, *J*=7.2 Hz, 1 H), 8.05 (d, *J*=7.2 Hz, 1 H).

8-Trifluoromethyl-3-cyclopropylmethyl-7-[(4-(2,4-difluorobenzyloxy)-1-piperidinyl)methyl]-1,2,4-triazolo[4,3-a]pyridine (23). Starting from **11** (0.140 g, 0.315 mmol) and 4-(2,4-difluorobenzyloxy)piperidine [C.A.S. 1121592-61-7] (0.095 g, 0.378 mmol), and following the procedure described for **12**, compound **23** was obtained (0.054 g, 36%). LCMS: *m/z* 481 $[M + H]^+$, t_R = 3.32 min. ^{1}H NMR (500 MHz, $CDCl_3$) δ ppm 0.30 - 0.40 (m, 2 H), 0.58 - 0.69 (m, 2 H), 1.12 - 1.23 (m, 1 H), 1.64 - 1.74 (m, 2 H), 1.89 - 2.01 (m, 2 H), 2.23 - 2.33 (m, 2 H), 2.70 - 2.79 (m, 2 H), 3.10 (d, *J*=6.6 Hz, 2 H), 3.43 - 3.51 (m, 1 H), 3.72 (d, *J*=1.7 Hz, 2 H), 4.55 (s, 2 H), 6.80 (td, *J*=9.5, 2.3 Hz, 1 H) 6.88 (td, *J*=8.2, 2.0 Hz, 1 H), 7.37 - 7.44 (m, 2 H), 8.04 (d, *J*=7.2 Hz, 1 H). M. p. 126.0 °C (B).

8-Trifluoromethyl-3-cyclopropylmethyl-7-[(*cis*-4-(2,4-difluorophenyl)-1-cyclohexylamino)methyl]-1,2,4-triazolo[4,3-a]pyridine (24). Starting from **9** (0.11 g, 0.409 mmol) and *cis*-4-(2,4-difluorophenyl)-, cyclohexylamine [C.A.S. 1374582-72-5] (0.103 g, 0.49 mmol) and following the procedure described for **13**, compound **24** was obtained (0.088 g, 46%). LCMS: *m/z* 465 $[M + H]^+$, t_R = 3.57 min. ^{1}H NMR (400 MHz, $CDCl_3$) δ ppm 0.29 - 0.41 (m, 2 H), 0.56 - 0.70 (m, 2 H), 1.12 - 1.24 (m, 1 H), 1.54 - 1.74 (m, 5 H), 1.75 - 1.93 (m, 4 H), 2.85 (tt, *J*=11.6, 3.2 Hz, 1 H), 2.96 - 3.03 (m, 1 H), 3.11 (d, *J*=6.7 Hz, 2 H), 4.01 (d, *J*=1.6 Hz, 2 H), 6.72 - 6.86 (m, 2 H), 7.15 - 7.23 (m, 1 H), 7.32 (d, *J*=7.2 Hz, 1 H), 8.08 (d, *J*=7.2 Hz, 1 H). M. p. 123.1 °C (B).

8-Trifluoromethyl-3-cyclopropylmethyl-7-[(*trans*-4-(2,4-difluorophenyl)-1-cyclohexyl)methyl]-1,2,4-triazolo[4,3-a]pyridine (25). Starting from **9** (0.11 g, 0.409 mmol) and *trans*-4-(2,4-difluorophenyl)cyclohexylamine [C.A.S. 1374582-80-5] (0.103 g, 0.49 mmol) and following the procedure described for **13**, compound **25** was obtained (0.085 g, 45%). LCMS: *m/z* 465 $[M + H]^+$, t_R = 3.27 min. ^{1}H NMR (400 MHz, $CDCl_3$) δ ppm 0.28 - 0.41 (m, 2 H), 0.57 - 0.70 (m, 2 H), 1.13 - 1.24 (m, 1 H), 1.24 - 1.37 (m, 2 H), 1.51 (qd, J=12.9, 2.8 Hz, 2 H), 1.58 (br s, 1 H), 1.84 - 1.96 (m, 2 H), 2.04 - 2.15 (m, 2 H), 2.57 (tt, *J*=11.1, 3.7 Hz, 1 H), 2.81 (tt, *J*=12.3, 3.2 Hz, 1 H), 3.11 (d, *J*=6.7 Hz, 2 H), 4.07 (d, *J*=1.8 Hz, 2 H), 6.70 - 6.85 (m, 2 H), 7.10 - 7.19 (m, 1 H), 7.34 (d, *J*=7.4 Hz, 1 H), 8.07 (d, *J*=7.2 Hz, 1 H). M. p. 110.1 °C (B).

8-Trifluoromethyl-3-cyclopropylmethyl-7-[(4-(2,6-difluorophenyl)-1-piperazinyl)methyl]-1,2,4-triazolo[4,3-a]pyridine (26). Starting from **11** (0.140 g, 0.315 mmol) and 2,6-difluorophenyl)piperazine [C.A.S. 255893-56-2] (0.089 g, 0.395 mmol), and following the procedure described for **12**, compound **26** was obtained (0.086 g, 60%). LCMS: *m/z* 452 $[M + H]^+$, t_R = 3.32 min. ^{1}H NMR (400 MHz, $CDCl_3$) δ ppm 0.30 - 0.42 (m, 2 H), 0.57 - 0.71 (m, 2 H), 1.14 - 1.24 (m, 1 H), 2.58 - 2.70 (m, 4 H), 3.11 (d, *J*=6.7 Hz, 2 H), 3.19 - 3.29 (m, 4 H), 3.80 (d, *J*=1.6 Hz, 2 H), 6.78 - 6.89 (m, 2 H), 6.89 - 6.99 (m, 1 H), 7.47 (d, *J*=7.2 Hz, 1 H), 8.07 (d, *J*=7.2 Hz, 1 H). M. p. 182.7 °C (B).

8-Trifluoromethyl-3-cyclopropylmethyl-7-[(4-(2,4-difluorophenyl)-1-piperazinyl)methyl]-1,2,4-triazolo[4,3-a]pyridine (27). Starting from **9** (0.1 g, 0.371 mmol) and 2,4-difluorophenyl)piperazine [C.A.S. 115761-79-0] (0.088 g, 0.446 mmol) and following the procedure described for **13**, compound **27** was obtained (0.107 g, 64%). LCMS: *m/z* 452 $[M + H]^+$, t_R = 3.16 min. ^{1}H NMR (500 MHz, $CDCl_3$) δ ppm 0.30 - 0.41 (m, 2 H), 0.58 - 0.69 (m, 2 H), 1.12 - 1.27 (m, 1 H), 2.63 - 2.75 (m, 4 H), 3.01 - 3.09 (m, 4 H), 3.10 (d, *J*=6.9 Hz, 2 H), 3.81 (d, *J*=1.4 Hz, 2 H), 6.76 - 6.85 (m, 2 H), 6.85 - 6.94 (m, 1 H), 7.40 (d, *J*=7.2 Hz, 1 H), 8.06 (d, *J*=7.2 Hz, 1 H). M. p. 141.5 °C (B).

8-Trifluoromethyl-3-cyclopropylmethyl-7-[(4-(2,4-dichlorophenyl)-1-piperazinyl)methyl]-1,2,4-triazolo[4,3-a]pyridine (28). Starting from **9** (0.085 g, 0.316 mmol) and 1-(2,4-dichlorophenyl)piperazine [C.A.S. 1013-78-1] (0.088 g, 0.379 mmol) and following the procedure described for **13**, compound **28** was obtained (0.063 g, 41%). LCMS: *m/z* 484 $[M + H]^+$, t_R = 3.87 min ^{1}H NMR (500 MHz, $CDCl_3$) δ ppm 0.27 - 0.41 (m, 2 H), 0.56 - 0.70 (m, 2 H), 1.14 - 1.24 (m, 1 H), 2.69 (t, *J*=4.6 Hz, 2 H), 3.07 (t, *J*=4.0 Hz, 2 H), 3.10 (d, *J*=6.9 Hz, 2 H), 3.81 (d, *J*=1.2 Hz, 2 H), 6.72 - 6.85 (m, 2 H), 6.86 - 6.95 (m, 1 H), 7.40 (d, *J*=7.2 Hz, 1 H), 8.06 (d, *J*=7.2 Hz, 1 H). M. p. 164.2 °C (B).

8-Trifluoromethyl-3-cyclopropylmethyl-7-[(4-(2,4-difluorophenyl)-1-diazepanyl)methyl]-1,2,4-triazolo[4,3-a]pyridine (29). Starting from **9** (0.1 g, 0.371 mmol) and 1-(2,4-difluorophenyl)-1,4-diazepane [C.A.S. 1065586-48-2] (0.095 g, 0.446 mmol) and following the procedure described for **13**, compound **29** was obtained (0.094 g, 55%). LCMS: *m/z* 466 $[M + H]^+$, t_R = 3.48 min. ^{1}H NMR (500 MHz, $CDCl_3$) δ ppm 0.30 - 0.41 (m, 2 H), 0.58 - 0.70 (m, 2 H), 1.14 - 1.24 (m, 1 H), 1.92 - 2.04 (m, 2 H), 2.74 - 2.81 (m, 2 H), 2.81 - 2.88 (m, 2 H), 3.10 (d, *J*=6.9 Hz, 2 H), 3.31 - 3.41 (m, 4 H), 3.90 (d, *J*=1.4 Hz, 2 H), 6.71 - 6.88 (m, 3 H), 7.41 (d, *J*=7.2 Hz, 1 H), 8.02 (d, *J*=7.2 Hz, 1 H). M. p. 108.0 °C (B).

ASSOCIATED CONTENT

Supporting Information

Atomic coordinates of the binding mode of **27** in the mGlu2 7TM homology model. Comparison of the binding mode of **6** (purple) and **27** (magenta). LCMS methods for the characterization of intermediate and final compounds. CEREP data for compound **27**. This material is available free of charge via the Internet at http://pubs.acs.org.

ACKNOWLEDGEMENTS

The authors thank collaborators from Addex Therapeutics, and the members of the purification and analysis group, the biology and in vitro metabolism team from Janssen R&D.

ABBREVIATIONS USED

AUC, area under the curve; AW, active wake, Cl, clearance; dSWS, deep non-REM sleep. EEG, electroencephalogram; F, oral bioavailailability; f_u, fraction unbound; GABA, γ-aminobutyric acid, GPCRs, G-protein coupled receptors; HLM, human liver microsomes; HP-β-CD, 2-hydroxylpropyl-beta-cyclodextrin; i.v., intravenous; Kin Sol, kinetic solubility; LAC, lowest active concentration; LAD, lowest active dose; lSWS, light non-REM sleep; mGlu2, metabotropic glutamate 2; n.t., not tested; PAM, positive allosteric modulator; Papp, apparent permeability; P-gp, P-glycoprotein; PK, pharmacokinetics; PW, passive wake; rt, room temperature; SAR, structure-activity relationship; SEM, standard error of mean; p.o., oral; REM, rapid eye movement; RLM, rat liver microsomes; s.c., subcutaneous; SD, standard deviation; sw-EEG, sleep-wake electroencephalogram; TM, Transmembrane.

AUTHOR INFORMATION

Corresponding Author: * To whom correspondence should be addressed. Tel: +34 925 245767. Fax: +34 925 245771. Email: jcid@its.jnj.com. Tel: +34 925 245779. Fax: +34 925 245771. Email: atrabanc@its.jnj.com.

Notes

The authors declare no competing financial interest.

REFERENCES

1 Pin, J. P.; Galvez, T.; Prezeau, L. Evolution, structure, and activation mechanism of family 3/C G-protein-coupled receptors. *Pharmacol. Ther.* **2003**, *98*, 325-354.

2 Brauner-Osborne, H.; Wellendorph, P.; Jensen, A. A. Structure, pharmacology and therapeutic prospects of family C G-protein coupled receptors. *Curr. Drug Targets* **2007**, *8*, 169-184.

3 Cartmell, J.; Schoepp, D. D. Regulation of neurotransmitter release by metabotropic glutamate receptors. *J. Neurochem.* **2000**, *75*, 889-907.

4 Johnson, M. P.; Barda, D.; Britton, T. C.; Emkey, R.; Hornback, W. J.; Jagdmann, G. E.; McKinzie, D. L.; Nisenbaum, E. S.; Tizzano, J. P.; Schoepp, D. D. Metabotropic glutamate 2 receptor potentiators: receptor modulation, frequency-dependent synaptic activity, and efficacy in preclinical anxiety and psychosis model(s). *Psychopharmacology* **2005**, *179*, 271-283.

5 Marek, G. J.; Behl, B.; Bespalov, A. Y.; Gross, G.; Lee, Y.; Schoemaker, H. Glutamatergic (N-methyl-D-aspartate receptor) hypofrontality in schizophrenia: too little juice or a miswired brain? *Mol Pharmacol.* **2010**, *77*, 317–326.

6 Chiechio, S.; Caricasole, A.; Barletta, E.; Storto, M.; Catania, M.V.; Copani, A.; Vertechi, M.; Nicolai, R.; Calvani, M.; Melchiorry, D.; Nicoletti, F. L-Acetylcarnitine induces analgesia by selectively upregulating mGlu2 metabotropic glutamate receptors. *Mol. Pharmacol.* **2002**, *61*, 989-996.

7 Chiechio, S.; Zammataro, M.; Morales, M. E.; Busceti, C. L.; Drago, F.; Gereau, R. W. 4th; Copani, A.; Nicoletti, F. Epigenetic modulation of mGlu2 receptors by histone deacetylase inhibitors in the treatment of inflammatory pain. *Mol. Pharmacol.* **2009**, *75*, 1014-1020.

8 Monn, J. A.; Valli, M. J.; Massey, S. M.; Wright, R. A.; Salhoff, C. R.; Johnson, B. G.; Howe, T.; Alt, C. A.; Rhodes, G. A.; Robey, R. L.; Griffey, K. R.; Tizzano, J. P.; Kallman, M. J.; Helton, D. A.; Schoepp, D. D. Design, synthesis, and pharmacologicalcharacterization of (+)-2-aminobicyclo[3.1.0]hexane-2,6-dicarboxylic Acid (LY354740): a potent, selective, and orally active group 2 metabotropic glutamate receptor agonist possessing anticonvulsant and anxiolytic Properties. *J. Med. Chem.* **1997**, *40*, 528-537.

9 Schoepp, D. D.; Wright, R. A.; Levine, L. R.; Gaydos, B.; Potter, W. Z. LY354740, an mGlu2/3 receptor agonist as a novel approach to treat anxiety/stress. *Stress* **2003**, *6*, 189−197.

10 Coffey, D. S.; Hawk, M. K.; Pedersen, S. W.; Vaid, R. K. An efficient synthesis of LY544344.HCl: a prodrug of mGluR2 agonist LY354740. *Tetrahedron Lett*. **2005**, *46*, 7299-7302.

11 Dunayevich, E.; Erickson, J.; Levine L.; Landbloom, R.; Schoepp, D. D.; Tollefson, G. D. Efficacy and tolerability of an mGlu2/3 agonist in the treatment of generalized anxiety disorder. *Neuropsychopharmacology* **2008**, *33*, 1603-1610.

12 Moher, E. D.; Monn, J. A. Prodrugs of excitatory amino acids. US7671082, 2010.

13 Monn, J. A. ; Massey, S. M.; Valli, M. J.; Henry, S. S.; Stephenson, G. A.; Bures, M.; Hérin, M.; Catlow, J.; Giera, D.; Wright, R. A.; Johnson, B. G.; Andis, S. L.; Kingston, A.; Schoepp, D.D. Synthesis and metabotropic glutamate receptor activity of S-oxidized variants of (−)-4-amino-2-thiabicyclo-[3.1.0]hexane-4,6-dicarboxylate: Identification of potent, selective, and orally bioavailable agonists for mGlu2/3 receptors. *J. Med. Chem.* **2007**, *50*, 233–240.

14 Patil, S. T.; Zhang, L.; Martenyi, F.; Lowe, S. L.; Jackson, K. A.; Andreev, B. V.; Avedisova, A. S.; Bardenstein, L. M.; Gurovich, I. Y.; Morozova, M. A.; Mosolov, S. N.; Neznanov, N. G.; Reznik, A. M.; Smulevich, A. B.; Tochilov, V. A.; Johnson, B. G.; Monn, J. A.; Schoepp, D. D. Activation of mGlu2/3 receptors as a new approach to treat schizophrenia: a randomized Phase 2 clinical trial. *Nature Med.* **2007**, *13*, 1102-1107.

15 Home page: https://investor.lilly.com/index.cfm . Lilly stops phase III development of pomaglumetad methionil for the treatment of schizophrenia based on efficacy results. https://investor.lilly.com/releaseDetail.cfm?ReleaseID=703018.Last accessed July 28th, 2016.

16 Marek G. J. When is a proof-of-concept (POC) not a POC? Pomaglumetad (LY2140023) as a case study for antipsychotic efficacy. *Curr. Pharm. Des.* **2015**, *21*, 3788-3796.

17 Kinon, B. J.; Millen, B. A.; Zhang, L.; McKinzie, D. L. Exploratory analysis for a targeted patient population responsive to the metabotropic glutamate 2/3 receptor agonist Pomaglumetad Methionil in schizophrenia. *Biol. Psych.* **2015**, *78*, 754-762.

18 Trabanco, A. A.; Cid, J. M.; Lavreysen, H.; Macdonald, G. J.; Tresadern, G. Progress in the development of positive allosteric modulators of the metabotropic glutamate receptor 2. *Curr. Med. Chem.* **2011**, *18*, 47-68.

19 Trabanco, A. A.; Cid, J. M. mGluR2 Positive Allosteric Modulators (PAMs): a patent review (2009-present). *Expert Opin. Ther. Patents* **2013**, *23*, 629-647.

20 Szabó, G,; Keserű, G. M. Positive allosteric modulators for mGluR2 receptors: A medicinal chemistry perspective. *Curr. Topics Med. Chem.* **2014**, *14*, 1771-1788.

21 Clayton, J.; Egle, I.; Empfield, J.; Folmer, J.; Isaac, M.; Ma, F.; Slassi, A. Oxadiazole derivatives and their use as metabotropic glutamate receptor potentiators. WO2008150233, 2008.

22 Home page: http://www.clinicaltrials.gov. The effects ADZ8529 on cognition and negative symptoms in schizophrenics. https://clinicaltrials.gov/show/NCT00986531 . Last accessed July 28th, 2016.

23 Home page: http://www.astrazeneca.com – Annual report 2010: https://www.astrazeneca.com/content/dam/az/our-company/investor-relations/presentations-and-webcast/Annual-Reports/2010-Annual-Report.pdf. Last accessed July 28th, 2016.

24 Home page: http://www.clinicaltrials.gov. The study of ADZ8529 for smoking cessation in female smokers. https://www.clinicaltrials.gov/ct2/show/NCT02401022?term=AZD8529&rank=1. Last accessed July 28th, 2016.

25 Home page: http://www.addextherapeutics.com. Addex reports top-line data from a successful phase 2a clinical study with ADX71149 in schizophrenia patients. http://www.addextherapeutics.com/investors/press-releases/news-details/article/addex-reports-top-line-data-from-a-successful-phase-2a-clinical-study-with-adx71149-in-schizophrenia/. Last accessed July 28th, 2016.

26 Home page: http://www.clinicaltrials.gov. Study to evaluate the efficacy and overall safety and tolerability of treatment with adjunctive JNJ 40411813 compared to placebo in patients with MDD with anxiety symptoms being treated with an antidepressant. http://clinicaltrials.gov/show/NCT01582815. Last accessed July 28th, 2016.

27 Kent, M. J.; Daly, E.; Kezic, I., Rossane, L.; Lim, P.; De Smedt, H.; De Boer, P; Van Nueten, L.; Drevets, W. C.; Ceusters, M. Efficacy and safety of an adjunctive mGlu2 receptor positive allosteric modulator to a SSRI/SNRI in anxious depression. Prog. *Neuro-psychopharmacol. Biol. Psych.* **2016**, *67*, 66–73.

28 Tresadern, G.; Cid, J. M; Macdonald, G. J.; Vega, J. A.; de Lucas, A. I.; García, A.; Matesanz, E.; Linares, M. L.; Oehlrich, D.; Lavreysen, H.; Biesmans, I.; Trabanco, A. A. Scaffold hopping from pyridones to imidazo[1,2-a]pyridines. New positive allosteric modulators of metabotropic glutamate 2 receptor. *Bioorg. Med. Chem. Lett.* **2010**, *20*, 175-179.

29 Trabanco, A. A; Tresadern, G.; Macdonald, G. J.; Vega, J. A.; de Lucas, A. I.; Matesanz, E.; Garcia, A.; Linares, M. L.; Alonso de Diego, S. A.; Alonso, J. M.; Oehlrich, D.; Ahnaou, A.; Drinkenburg, W.; Mackie, C., Andres, J. I. ; Lavreysen, H.; Cid, J. M. Imidazo[1,2-a]pyridines: Orally active positive allosteric modulators of the metabotropic glutamate 2 receptor. *J. Med. Chem.* **2012**, *55*, 2688-2701.

30 Cid-Nuñez, J. M.; Trabanco-Suárez, A. A.; Macdonald, G. J. Preparation of indole and benzoxazine derivatives as modulators of metabotropic glutamate receptors for treating neurological and psychiatric disorders. WO 2010060589 A1, 2010.

31 Trabanco-Suárez, A. A.; Tresadern, G. J.; Vega-Ramiro, J. A.; Cid-Nuñez, J. M. Preparation of imidazopyridine derivatives for use as mGluR2 receptor modulators. WO2009062676 A2, 2009.

32 Cid, J. M.; Tresadern, G.; Vega, J. A.; De Lucas, A. I.; Matesanz, E.; Iturrino, L.; Linares, M. L.; García, A.; Andrés, J. I.; Macdonald, G. J.; Oehlrich, D.; Lavreysen, H.; Megens, A.; Ahnaou, A.; Drinkenburg, W.; Mackie, C.; Pype, S.; Gallacher, D.; Trabanco, A. A. Discovery of 3-cyclopropylmethyl-7-(4-phenyl-piperidin-1-yl)-8-trifluoromethyl[1,2,4]triazolo[4,3a] pyridine (JNJ-42153605): A positive allosteric modulator of the metabotropic glutamate 2 receptor. *J. Med. Chem.* **2012**, *55*, 8770-8789.

33 Tresadern, G.; Cid, J. M.; Trabanco, A. A. QSAR design of triazolopyridine mGlu2 receptor positive allosteric modulators. *J. Mol. Graph. Model.* **2014**, *53*, 82-91.

34 Ahnaou, A.; Lavreysen, H.; Tresadern, G.; Cid, J. M.; Drinkenburg, W. H. mGlu2 receptor agonism, but not positive allosteric modulation, elicits rapid tolerance towards their primary efficacy on sleep measures in rats. *PLoS One* **2015**, *10*, e0144017.

35 Doornbos, M. L. J.; Pérez-Benito, L.; Tresadern, G.; Mulder-Krieger, T.; Biesmans, I.; Trabanco, A. A.; Cid, J. M.; Lavreysen, H.; IJzerman, A. P.; Heitman, L.H. Molecular mechanism of positive allosteric modulation of the metabotropic glutamate receptor 2 by JNJ-46281222. *Br. J. Pharmacol.* **2016**, *173*, 588-600.

36 Farinha, A.; Lavreysen, H.; Peeters, L.; Russo, B.; Masure, S.; Trabanco, A. A.; Cid, J.; Tresadern, G. Molecular determinants of positive allosteric modulation of the human metabotropic glutamate receptor 2. *Br. J. Pharmacol.* **2015**, *172*, 2383-2396.

37 Bennett, K. A.; Doré, A. S.; Christopher, J. A.; Weiss, D. R.; Marshall, F. H. Structures of mGluRs shed light on the challenges of drug development of allosteric modulators. *Curr. Opin. Pharmacol.* **2015**, *20*, 1-7.

38 Radioligand binding assays at CEREP were conducted using standard protocols (details can be found under http://www.cerep.fr/cerep/users/pages/catalog/General/catalog.asp).

39 Cid, J. M.; Tresadern, G.; Duvey, G.; Lütjens, R.; Finn, T.; Rocher, J. P.; Poli, S.; Vega, J. A.; de Lucas, A. I.; Matesanz, E.; Linares, M. L.; Andrés, J. I.; Alcazar, J.; Alonso, J. M.; Macdonald, G. J.; Oehlrich, D.; Lavreysen, H.; Ahnaou, A.; Drinkenburg, W.; Mackie, C.; Pype, S.; Gallacher, D.; Trabanco, A. A. Discovery of 1‑butyl-3-chloro-4-(4-phenyl-1-piperidinyl)- (1H)‑pyridone (JNJ-40411813): A novel positive allosteric modulator of the metabotropic glutamate 2 receptor. *J. Med. Chem.* **2014**, *57*, 6495−6512.

40 Ahnaou, A.; Dautzenberg, F. M.; Geys, H.; Imogai, H.; Gibelin, A.; Moechars, D.; Steckler, T.; Drinkenburg, W. H. Modulation of group II metabotropic glutamate receptor (mGlu2) elicits common changes in rat and mice sleep−wake architecture. *Eur. J. Pharmacol*. **2009**, *603*, 62−72.

41 Feinberg, I.; Campbell, I. G.; Schoepp, D. D.; Anderson, K. The selective group mGlu2/3 receptor agonist LY379268 suppresses REM sleep and fast EEG in the rat. *Pharmacol., Biochem. Behav*. **2002**, *73*, 467−474.

42 Doré, A. S.; Okrasa, K.; Patel, J. C.; Serrano-Vega, M.; Bennett, K.; Cooke, R. M.; Errey, J. C.; Jazayeri, A.; Khan, S.; Tehan, B. Structure of class C GPCR metabotropic glutamate receptor 5 transmembrane domain. *Nature* **2014**, *511*, 557–562.

43 Wu, H.; Wang, C.; Gregory, K. J.; Han, G. W.; Cho, H. P.; Xia, Y.; Niswender, C. M.; Katritch, V.; Meiler, J.; Cherezov, V. Structure of a class C GPCR metabotropic glutamate receptor 1 bound to an allosteric modulator. *Science* **2014**, *344*, 58–64.

44 Rasmussen, S. G. F.; DeVree, B. T.; Zou, Y.; Kruse, A. C.; Chung, K. Y.; Kobilka, T. S.; Thian, F. S.; Chae, P. S.; Pardon, E.; Calinski, D. Crystal structure of the β2 adrenergic receptor–Gs protein complex. *Nature* **2011**, *477*, 549–555.

45 Maestro *v10.3* (Schrodinger LLC, New York, NY, USA).

46 Abraham, M. J.; Murtola, T.; Schulz, R.; Páll, S.; Smith, J. C.; Hess, B.; Lindahl E. GROMACS: High performance molecular simulations through multi-level parallelism from laptops to supercomputers. *SoftwareX* **2015**, *1-2*, 19-25.

47 Cordomí, A.; Edholm, O.; Perez, J. J. Effect of force field parameters on sodium and potassium ion binding to dipalmitoyl phosphatidylcholine bilayers. *J. Chem. Theory Comput*. **2009**, *5*, 2125–2134.

48 Joosten, R. P.; te Beek, T. A. H.; Krieger, E.; Hekkelman, M. L.; Hooft, R. W. W.; Schneider, R.; Sander, C.; Vriend, G. A series of PDB related databases for everyday needs. *Nucleic Acids Res*. **2011**, *39*, D411–9.

49 Bussi, G.; Donadio, D.; Parrinello, M. Canonical sampling through velocity rescaling. *J. Chem. Phys*. **2007**, *126*, 014101.

50 Miyamoto, S.; Kollman, P. A. Settle: An analytical version of the SHAKE and RATTLE algorithm for rigid water models. *J. Comput. Chem*. **1992**, *13*, 952–962.

51 Darden, T.; York, D.; Pedersen, L. Particle mesh Ewald: An N·log(N) method for Ewald sums in large systems. *J. Chem. Phys*. **1993**, *98*, 10089.

52 Lindorff-Larsen, K.; Piana, S.; Palmo, K.; Maragakis, P.; Klepeis, J. L.; Dror, R. O.; Shaw, D. E. Improved side-chain torsion potentials for the Amber ff99SB protein force field. *Proteins* **2010**, *78*, 1950–1958.

53 Berger, O.; Edholm, O.; Jähnig, F. Molecular dynamics simulations of a fluid bilayer of dipalmitoylphosphatidylcholine at full hydration, constant pressure, and constant temperature. *Biophys. J*. **1997**, *72*, 2002–2013.

54 Bayly, C. I.; Cieplak, P.; Cornell, W.; Kollman, P. A. A well-behaved electrostatic potential based method using charge restraints for deriving atomic charges: the RESP model. *J. Phys. Chem*. **1993**, *97*, 10269–10280.

55 Cordomí, A.; Caltabiano, G.; Pardo, L. Membrane protein simulations using AMBER force field and Berger lipid parameters. *J. Chem. Theory Comput.* **2012**, *8*, 948–958.